# Synthesis and Properties of Mono-Substituted Liquid Crystalline Polyacetylene Derivatives – Doping, Magnetic Orientation, and Photo-isomerization

Hiromasa Goto[a], Shigeki Nimori[b], Kazuo Akagi*[a]

[a]Tsukuba Research Center for Interdisciplinary Materials Science (TIMS), Institute of Materials Science, University of Tsukuba, Tsukuba, Ibaraki 305-8573, Japan. E-mail: akagi@ims.tsukuba.ac.jp

[b]Tsukuba Magnet Laboratory, National Research Institute for Metals, Tsukuba, Ibaraki 305-0003, Japan

***Keywords:*** Liquid crystals; Polyacetylene; Polymer; Photo-induced isomerization, Magnetic orientation

**Abstract**

Mono-substituted acetylene monomers with a liquid crystalline (LC) group are polymerized using rhodium, iron or molybdenum complex catalysts. LC polyacetylene derivatives with number-averaged molecular weights of 4000–330000 were obtained in 5–92% yield. The LC behavior is examined by X-ray diffraction, differential scanning calorimetry, and polarizing optical microscopy. The polymers prepared using rhodium or iron catalyst are confirmed to assume a *cis* form and to undergo an irreversible isomerization to the *trans* form upon heating. Photo-responsive polyacetylene derivatives are successfully synthesized through the introduction of an azobenzene moiety as a mesogenic core into the side-chain, and these forms exhibit a reversible photochemical *cis*-to-*trans* isomerization of the azobenzene moiety.

## 1. Introduction

Conjugated polymers exhibit electrical transport, nonlinear optical (NLO) , and organic magnetic phenomena. Iodine-doped polyacetylene in particular, regarded as a representative organic conductor, has electrical conductivity comparable to metals. This high conductivity has also been achieved in macroscopically aligned polyacetylene films. In 1987, a directly aligned polyacetylene film using liquid crystal (LC) as a solvent under a magnetic field was synthesized [1]. It has been confirmed through scanning electron microscopy that the high conductivity of this highly oriented polyacetylene is due to the strongly aligned fibril morphology. LC ordering is thus considered to provide an effective and useful anisotropic environment for polymer synthesis.

LC is unique in that it exhibits both crystal-like birefringence and fluid behavior. Conjugated polymers with LC side-chains are intriguing classes of polymer [2]. In the side-chain LC conjugated polymer, the side-chain array in the LC state induces spontaneous orientation of the polymer, which may be attended to improve the main-chain coplanarity. Furthermore, through the application of an external force, such as shear stress or an electric/magnetic field, the orientation can be controlled on a macroscopic scale.

In the present study, polyacetylenes bearing various types of functional LC are synthesized, and the liquid crystallinity, doping effects, magnetic orientation, and photo-induced isomerization are examined as an exploration of the potential of liquid crystalline conjugated polymers.

## 2. Synthesis

*2-1. Monomer Synthesis*

The syntheses of 5-[*4*-(*trans*-4’-*n*-alkylcyclohexyl)phenoxy]-1-pentyne, 1-[4-(*trans*-4’-pentylcyclohexyl)phenoxy]-6-bromohexane, and 5-(4-pentyl-4’-biphenoxy)-1-pentyne were carried out by the method described in the literature [3, 4(e)]. Here, the three monomers are denoted PCHR03A, PCH506Br, and BP503A, respectively, where P denotes phenyl, CH denotes cyclohexyl, R is the carbon number of terminal alkyl groups, 0 is ether oxygen, 3 (6) is the carbon number of flexible alkyl spacers, A denotes acetylene, Br denotes bromine connected to alkyl spacer, and BP denotes biphenyl.

The coupling reaction between sodium acetylide and PCH506Br in *N*,*N*’-dimethylformamide (DMF) afforded PCH506A in 10% yield (Scheme 1).

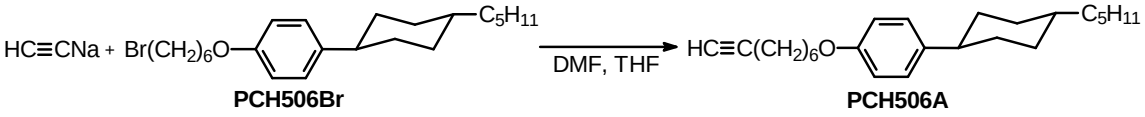


**Scheme 1**

CB03A was prepared via Williamson reaction by etherification between 4'-hydroxy-biphenyl-4-carbonitrile and 5-chloro-1-pentyne in the presence of potassium iodide as a catalyst (Scheme 2).

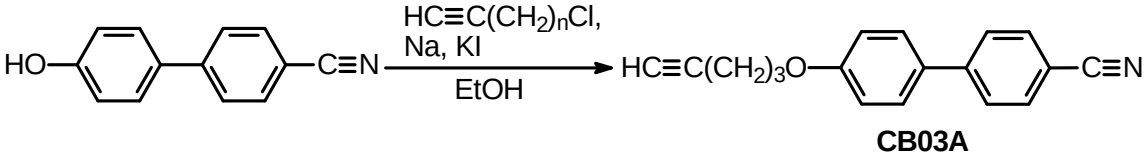


**Scheme 2**

The synthetic route to PCH5C010A (5-carbon terminal alkyl group, C0: ester group, 10-carbon flexible alkyl spacer) is described in Scheme 3. PCH5C010A was prepared via Mitsunobu reaction by esterification between tridec-12-ynoic acid and 4-(*trans*-4'-*n*-pentylcyclohexyl)phenol (PCH500) using diethylazodicarboxylate (DEAD) and triphenyl phosphine (TPP).

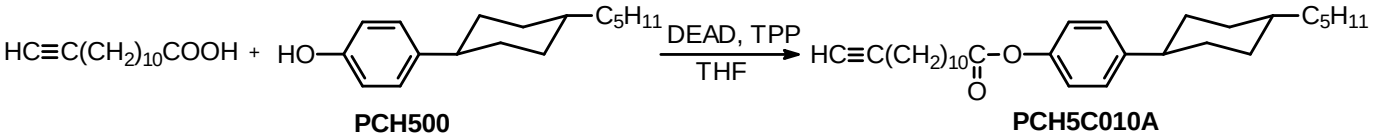


**PCH500** **PCH5C010A**

**Scheme 3**

10-Bromodecan-1-ol was converted to 10-bromodecan-1-chloride using $SOCl_2$ and then coupled with sodium acetylide to afford **2**. Subsequently, compound **2** was coupled with PCH500 to afford PCH5010A with a long alkyl spacer (Scheme 4).

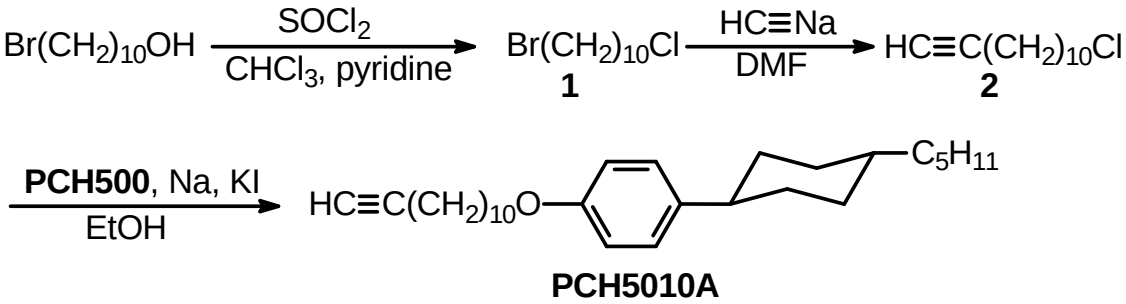


**PCH5010A**

**Scheme 4**

An acetylene monomer with azomethine (AM) LC group was prepared via the synthetic route described in Scheme 5. 4-Hydroxybenzaldehyde and 5-chloro-1-pentyne were coupled using

sodium in the presence of potassium iodide by Williamson etherification in ethanol to afford **3**. Compound **3** was then coupled with an equi-molar amount of 4-*n*-butylaniline to give AM403A (4-carbon terminal group, 3-carbon spacer).

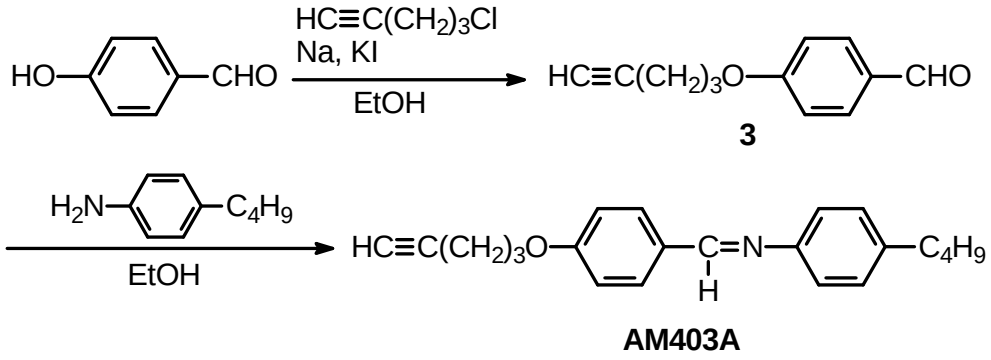


**Scheme 5**

Scheme 6 describes the synthetic route to the acetylene monomer with azobenzene (AB) LC group. The azo-coupling reaction of 4-butylaniline with phenol was carried out to give AB40 (4-carbon terminal alkyl group). In the next step, AB40 and 5-chloro-1-pentyne were coupled in the same manner as in the preparation of AM403A to afford the desired monomer AB403A.

The monomers were characterized by elemental analysis, $^{1}$H nuclear magnetic resonance (NMR), $^{13}$C NMR, and infrared (IR) absorption spectroscopy to confirm chemical structures. Selected samples were further investigated by $^{13}$C–$^{1}$H NMR-correlated two-dimensional spectroscopy to confirm the structures.

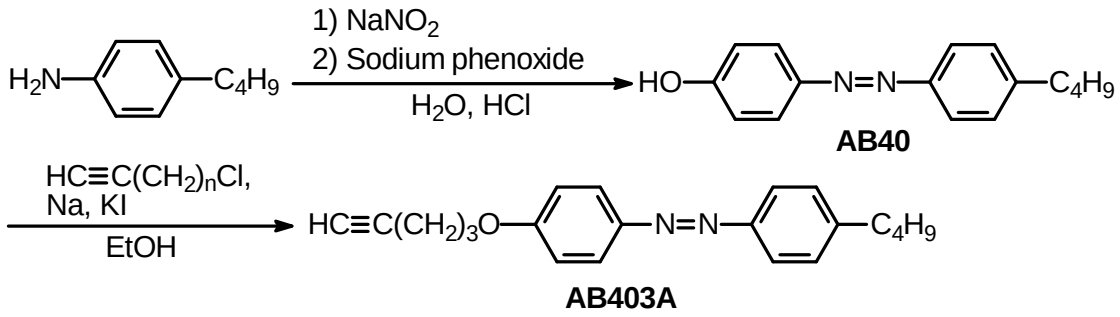


**Scheme 6**

*2-2. Polymerization*

Polymerization was conducted in a Schlenk flask equipped with a three-way stopcock under an argon atmosphere at room temperature. The acetylene derivatives were polymerized as monomers using three types of metal complex catalysts: $[Rh(NBD)Cl]_2$-$Et_3N$ (Wilkinson-type, where NBD denotes norbornadiene, and $Et_3N$ is triethylamine), $Fe(acac)_3$-$Et_3Al$ (Zieglar-Natta-type, where acac denotes acetylacetonate and $Et_3Al$ is triethylaluminum), and $MoCl_5$-$Ph_4Sn$ (metathesis-type, where $Ph_4Sn$ is tetraphenyl tin). The molecular structures of the polymers are summarized in Scheme 7. A typical polymerization procedure using the Rh complex catalyst was as follows. In a Schlenk tube, 2.1 mg (0.045 mmol) of $[Rh(NBD)Cl]_2$ was added to 1 mL of $Et_3N$ with stirring under an argon atmosphere. After aging for 30 min, 1.41 g (4.5 mmol) of the PCH503A monomer in 1.8 mL of tetrahydrofuran (THF) was added dropwise to the solution. After stirring for 24 h at room temperature, the reaction mixture was dissolved in a minimal amount of THF, then poured into a large volume of methanol. The solution was thoroughly washed with methanol to dissolve and completely remove the catalyst and the fractions of low molecular weight. The solution was filtered

off and the filtrate dried under vacuum to afford a yellow powder as the desired polymer. The polymer was soluble in THF and $CHCl_3$. The polymer yield decreased with an increase in the monomer/catalyst ratio (Table 1). However, the number-average molecular weight ($M_n$) reached a maximum at a monomer/catalyst ratio of 1000.

Bulk polymerization was also carried out using the Rh catalyst. In this procedure, the PCH503A monomer (0.31 g, 1 mmol) was charged in a Schlenk flask, to which 2 drops of the Rh catalyst in $Et_3N$ solution (0.01 M) was added. The weight-average molecular weight ($M_w$) of the polymer increased to 170000 after 6 min, accompanied by a broadening of the molecular weight distribution (MWD) to 6.8.

Typical procedures using the Fe or Mo catalyst were as follows. A catalyst solution was prepared by dissolving $Fe(acac)_3$ (0.01 g, 0.03 mmol) or $MoCl_5$ (0.01 g, 0.03 mmol) with 2.2 mL of toluene in a Schlenk tube under an argon atmosphere and constant stirring. $Et_3Al$ (0.025 mL, 0.18 mmol) in the case of $Fe(acac)_3$ and $Ph_4Sn$ (0.006 g, 0.015 mmol) in the case of $MoCl_5$ was added to the solution at room temperature. After stirring for 30 min, 3 mmol of the monomer was added to the solution. Polymerization was conducted at room temperature for 24 h, and the reaction was terminated by pouring the mixture into a large volume of methanol. The polymer was filtered off, and the filtrate dried under reduced pressure. Polymers prepared using the Rh, Fe, and Mo catalysts are denoted PPCHR03A(Rh,Fe,Mo).

The polymerization yield and molecular weight evaluated by gel permeation chromatography (GPC) relative to a polystyrene (PS) standard are summarized in Table 2. The Fe-based polymers

were only partially insoluble due to the high molecular weight. It is noteworthy that CB03A with the cyano group could not be polymerized by $Fe(acac)_3$-$Et_3Al$, attributable to the -CN moiety, which behaves as a catalytic poison for $Et_3Al$. Therefore, $(CH_3)_2S{\cdot}BH_3$ was employed as a cocatalyst for $Fe(acac)_3$ in place of $Et_3Al$. Polymerization of the monomer with the cyano moiety using the boron complex was successful, affording the corresponding polymer PCB03A(Fe). However, this catalytic system gave a somewhat low ($M_n = 4000$) molecular weight for PCB03A. A polymer bearing an azomethine LC substituent prepared using the $Fe(acac)_3$ catalyst, PAM403A(Fe), was insoluble in common solvents such as THF and chloroform due to its very high molecular weight, yet displayed a colorful fan-shaped smectic texture under polarizing optical microscopy (POM). The polymers prepared by the Mo catalyst had an $M_n$ of $1.2–6.7 \times 10^4$, whereas those catalyzed by $Fe(acac)_3$-$Et_3Al$ had much higher molecular weight ($M_n = 12.0–33.0 \times 10^4$).

## 3. Characterization

### *3.1. Chemical structure*

Figure 1 shows the IR spectra of the CB03A monomer and PCB03A(Rh) polymer. The IR spectrum of the polymer does not exhibit absorptions characteristic to the acetylenic moiety in the monomer (e.g., ≡C–H stretching at 3300 $cm^{-1}$, C≡C stretching at 2100 $cm^{-1}$, ≡C–H out-of-plane vibration near 690 $cm^{-1}$). However, the IR spectra of the polymers were otherwise similar to those of the corresponding monomers.

Figure 2 shows the $^{13}C$ NMR spectra of AB403A monomer and PAB403A(Rh) polymer. The

acetylenic carbons of the monomer are shifted to the lower magnetic region after polymerization.

The molecular structure of PPCH503A(Rh) was confirmed by $^{13}C$ $^{1}$–H correlation spectroscopy (COSY) NMR (Figure 3). Signals due to carbon were identified in the $^{13}C$ NMR spectrum (b, i, and f at 138.9, 139.5, and 157.1 ppm). Peaks in the $^{13}C$ NMR spectrum characteristic of olefin carbons were observed at 119.7 and 138.9 ppm in the polymer instead of 68.7 and 83.6 ppm due to acetylenic carbon in the monomer. This result indicated that opening of the acetylenic C≡C bond in the monomer was catalyzed by Rh to give a linear polymer with conjugated double bonds. The peak at 5.9 ppm, characteristic of the proton attached to the *cis* sequence of the double bond, is observed in the $^{1}H$ NMR spectrum of the predominantly *cis* polyacetylene derivative [4]. This $^{1}H$ NMR signal correlates to the signal at around 120 ppm in the $^{13}C$ NMR spectrum. Polymers prepare using the Fe and Rh catalysts exhibit a signal attributable to the olefin proton at around 6 ppm in the $^{1}H$ NMR spectrum, indicating the predominance of the *cis* form in these preparations. The Mo catalyst predominantly afforded the *trans* form of the polymers (no signal at 6 ppm). Olefin proton of *cis* form of other polymers was confirmed by NMR measurements (Table 2). In the ultraviolet-visible (UV-vis) absorption spectra of the PCH503A monomer and PPCH503A(Rh) polymer in THF solution, the absorption band at 270 nm is considered to the π–π* transition of the benzene ring in the mesogen, while the absorption at 320 nm is attributable to the π-π* transition of the conjugated double bonds of the main-chain. Polymers prepared using the Fe and Rh catalysts display an absorption peak at 320 nm, while those prepared using the Mo catalyst exhibit an absorption

shoulder in the same region.

*3.2. Liquid crystallinity and cis-trans isomerization*

All of the polymers produced in this study exhibit liquid crystallinity except for PCH203A and PCB03A prepared using $Fe(acac)_3$-$(CH_3)_2S{\cdot}BH_3$. Although the melting point of PCB03A(Fe) is around 200 °C, this form does not display birefringence under POM. In the case of AB403A monomer, it is evident from the Schlieren texture observed in the monomer that the liquid crystalline phase is nematic. The monomer displays monotropic liquid crystalline behavior, while the polymer exhibits a micro-polygonal smectic texture.

PPCH803A polymer displays a bâtonnets texture and fan-shaped smectic texture upon cooling, whereas the monomer (PCH803A) exhibits only a nematic phase. This can be due to the arrangement of the mesogenic side-chains with the aid of the polyacetylene main-chain as a guide, which allows the side-chains to form a smectic array. The other monomers and polymers exhibit the same tendency.

Notably, while the PCH303A monomer (3-carbon spacer, 3-carbon terminal alkyl group) does not display liquid crystallinity, the PPCH303A(Mo) polymer assumes a clear fan-shaped texture of smectic LC, which is of a higher order than the nematic phase. This phenomenon may be referred to so as a polymer effect. In the liquid crystalline polymers, the spacer length plays an important role [5], altering the properties of the liquid crystalline state. In the case of polyethylene-type polymers (non-conjugated polymers), longer spacer lengths result in more stable mesophases by providing

effective decoupling between the polymer main-chain and the mesogen group. PPCH5C010A and PPCH5010A, both with long alkyl spacers (C = 10), exhibit birefringence, but contain only very small LC domains. In contrast, PPCH303A, PPCH503A, PPCH603A, PPCH703A, PPCH803A (3-carbon spacer), and PPCH506A (6-carbon spacer) display distinct large LC domains under POM. This result suggests that the interaction between the mobility of the mesogenic substituent, related to the flexibility of the alkyl spacer, and the stiffness of the polyene main-chain leads to stable smectic ordering of the entire polymer system. These polymers are thus able to form higher-ordered structures through spontaneous orientation within the domains of the smectic phase.

PPCH003A, which does not contain a terminal alkyl group in the mesogen, and PPCH203A, which has a short terminal alkyl group in the mesogen, do not display liquid crystallinity. Polymers with mesogenic groups having terminal alkyl groups longer than ethylene (>2), on the other hand, they exhibit liquid crystallinity. The domain size of the LC phase increases with the length of the terminal alkyl chain in the side-chain, implying that the terminal alkyl group also plays an important role in stabilizing the LC in the polymer.

Conoscope observation of the homeotropic (perpendicular to the glass slide) region of PPCH503A(Rh) gives Maltese cross image. Color upon insertion of a 1/4 wavelength plate, black second and fourth quadrants, and blue first and third quadrants; yellow second and fourth quadrants upon insertion of a gypsum first-order red plate demonstrate that the polymer is an optically positive uniaxial material (see supplementary data) [6]. The symmetry of the Maltese cross indicates that the mesogenic side-chains have no tilt-angle with respect to the glass substrate. These

results suggest that the mesophase of PPCH503A(Rh) is smectic A (SmA).

During differential scanning calorimetry (DSC) measurements, the large exothermic signal appeared in the first heating process, which is due to *cis*-to-*trans* isomerization of the main-chain. Polymers prepared using the Mo catalyst do not exhibit this *cis*-to-*trans* isomerization in the first heating scan because the Mo catalyst produces *trans*-polyacetylene. No signal due to transition to the mesophase was observed in the first heating process for polymers prepared using either Rh or Fe. The exothermic signal in the first heating scan corresponds to the $^{1}$H NMR signal due to olefin proton of the *cis*-form at around 6 ppm (Table 2). Prior to heating, the polymer is predominantly in the *cis* (*cis*-*cisoidal* or *cis*-*transoidal*) form. Heating causes thermal isomerization of the polymer, resulting in a conformational change from the *cis* to the *trans* (*trans*-*transoidal*) form. The polymer exhibited a mesophase in both the second heating and the first cooling processes, indicating that the *trans* form of the polymer has enantiotropic liquid crystallinity.

In the case of PPCH803A(Fe), the polymer was isomerized from the *cis* to the *trans* form in the first heating process, but the temperature range of the mesophase was lower in the first cooling and second heating processes than for the *trans* PPCH803A(Mo). Thermal treated PPCH803A(Fe) can have low viscosity and relatively low molecular weight ($M_n \cong 4000$) due to scission of the main-chain during the *cis*-to-*trans* isomerization process. PPCH503A(Fe) exhibits the same tendency in this regard as PPCH803A(Fe) .

X-ray diffraction (XRD) measurements reveal two diffraction peaks: a sharp peak at a low angle and a broad peak at a high angle. This type of XRD pattern is usually encountered for smectic

phases. These low-angle and high-angle diffractions correspond to interlayer and inter-side-chain distances of 37.5 and 4.7 Å. This analysis suggests a polymer structure in which the LC side-chains are alternately located on either side of the polyene chain (both-sided structure) to form head-to-head/tail-to-tail linkages. These assignments are supported by molecular mechanics (MM) calculations, which give distances of 41.0 and 5.0 Å, as both-sided structure, respectively. The polymer structure also indicates that the LC side-chains have no tilt with respect to the main-chain, leading to a typical SmA structure. A plausible structure for the polymer in the smectic LC state is shown in Figure 4. In this case, the LC molecules aggregate into a layer structure, and the polyene forms a pseudo-layer structure accompanying the smectic LC order. In the case of PAB403A, the interlayer and inter-side-chain distances were 39.2 (calcd: 39 Å in *trans* form of azobenzene, as both-sided structure) and 4.4 Å (calcd: 4.0 Å in *trans* form of azobenzene), respectively. This result indicates that PAB403A with the azobenzene mesogenic group also forms a both-sided structure.

As the *cis* form was found in DSC to be thermally unstable and readily isomerize to the *trans* form during the first heating process, the formation was further investigated by heating of the polymer under argon for 10 min. The IR spectra of the polymer after heat treatment are shown in Figure 5. The intensity of the absorption band at 965 $cm^{-1}$ increases with the temperature of heating, consistent with the DSC results. This absorption band is thus considered to be due to a C–H out-of-plane deformation vibration of the *trans* polyene main-chain. The LC-substituted acetylene monomers approaching catalytically active sites are polymerized via a sequence of head-to-head and tail-to-tail linkages, yielding the stereoregular *cis* form [7]. The *cis* form is a kinetic product and

hence upon heating is converted to the thermodynamic *trans* form.

**4. Gas-phase doping**

*In-situ* gas-phase doping of the polymer with iodine was performed to investigate the interaction between the main-chain and the dopant. As the gas-phase iodine doping proceeded, the absorption band at 320 nm assignable to the π-π* transition of the polyene chain gradually weakened, accompanied by the growth of an absorption band at around 400 nm and weakening of a new band at around 700 nm. In the course of doping, two isosbestic points were observed, at 355 and 655 nm (supplementary data). These spectroscopic features suggest the existence of molecular interaction under equilibrium, probably due to a charge transfer reaction between the polyacetylene derivative and the iodine dopant. The results of the present experiment are consistent with the results of Masuda and Higashimura, who evaluated the formation of the charge transfer-type complex of polyphenylacetylene with low molecular weight electron acceptors, such as dichlorodicyanoquinone (DDQ), 7,7',8,8'-tetracyanoquinodimethane (TCNQ), bromine, and antimony pentachloride [8].

The same *in-situ* doping of the polymer was also performed using $AsF_5$ (Figure 6). The strong dopability of $AsF_5$ resulted in a more drastic change in the absorption spectra. At the start of the doping process, a new and extremely broad absorption band emerged, the band edge of which extended into the near-infrared region. A new absorption band at 370 nm grew rapidly with continued doping, accompanied by the emergence of a shoulder at 450 nm and a broad band centered around 520 nm. Although the specific assignments of these new bands remain to be

confirmed, it is evident that not only iodine but also $AsF_5$ are suitable for the chemical doping of liquid crystalline polyacetylene derivatives with larger ionization potentials compared to unsubstituted polyacetylene. These results confirm the feasibility of chemical doping for the present polymer series.

**5. Orientation of the polymer by application of an external magnetic field**

Control of the polymer orientation by application of an external magnetic field was investigated using PPCH503A(Rh). The polymer was melted and then gradually cooled to the mesophase under a magnetic field of 10 Tesla generated by a superconducting magnet. The liquid crystalline domains aligned parallel to the magnetic field to form a mono-domain structure. Figure 7 shows POM images of the non-aligned and aligned polymer films, which both exhibit fan-shaped textures. Figure 8 shows the XRD pattern of the aligned polymer film. The side-chains of the polymer spontaneously orientate in the liquid crystalline state to form a multi-domain structure. However, after application of an external magnetic field (10 T, 30 min), all domains became aligned in a single direction parallel to the magnetic field vector.

**6. Photo-induced isomerization of side-chains**

Azobenzene is a well-known photosensitive chromophore, and the azobenzene moiety undergoes photo-induced reversible isomerization. Oh et al. independently synthesized polyacetylene derivative with azobenzene units [9]. Teraguchi and Masuda prepared a polyacetylene directly

connected with an azobenzene moiety, and confirmed the *cis*-to-*trans* isomerization of the side-chain upon irradiation with UV or visible light [10]. Soluble functional polyacetylene copolymer containing azobenzene as a NLO chromophore was synthesized [11].

The photosensitive LC polyacetylene derivative prepared in the present study has an azobenzene as a mesogenic core and a photo-isomerization moiety, and which is connected to the main-chain via alkylene spacing groups.

Figure 9 shows changes in the UV-vis absorption spectra for PAB403A(Rh) in THF during irradiation with UV or visible light. The absorptions at both 345 nm ($\pi$-$\pi^*$ transition) due to the *trans* form and 240 nm due to the disubstituted phenylene ring weakened upon irradiation with UV light, accompanied by a gradual strengthening of the 440 nm band (n-$\pi^*$ transition) due to the *cis* form [12]. Subsequent irradiation with visible light caused an increase in the intensity of the 240 and 345 nm bands, and a weakening of the 440 nm band. These results imply that a reversible *cis*-to-*trans* isomerization of the azobenzene moiety occurs under UV and visible light irradiation. However, the POM image shows that this transformation is not accompanied by distinct changes in texture, despite the occurrence of isomerization in the solid state at room temperature. This suggests that the higher-order structure of the polymer is not notably affected by the microscopic structural changes localized on the side-chain. In other words, the smectic phase characterized by the macroscopic optical texture remains unchanged during the local distortion caused by *cis*-to-*trans* isomerization in the azobenzene moiety of the side-chain.

**7. Conclusions**

We synthesized polyacetylene derivatives bearing various types of LC substituent. Seventeen polymers showed thermotropic smectic phase. Magnetic orientation of the LC polyacetylene was successfully carried out, and its alignment was confirmed through polarizing optical microscopy observation and XRD measurement. Moreover, photo-induced isomerization of polyacetylene derivative bearing azobenzene LC group was examined. These results may provide further possibility to both conjugated polymer and liquid crystal research field.

## 8.Experimental

### *8-1. Techniques*

All $^{1}H$ NMR and $^{13}C$ NMR spectra were measured with a BRUKER AM500 FT-NMR spectrometer. $^{13}C$-$^{1}H$ NMR was obtained by COSY ($^{13}C$-$^{1}H$ hetero shift correlation spectroscopy) method for confirmation of the structure. $CDCl_3$ was used as a deuterated solvent, and tetramethylsilane (TMS) was used as an internal standard. Infrared spectroscopic measurement was carried out with a JASCO FT-IR 550 spectrometer using KBr method. Elemental analysis were recorded on a Perkin-Elmer 2400 CHN Elemental Analyzer at Chemical Analysis Center, University of Tsukuba. Phase transition temperatures were determined using a Perkin-Elmer differential scanning calorimeter (DSC 7) and a TA instrument Q100 DSC apparatus at a constant heating/cooling rate of 10°C/min, where first heating, first cooling and second heating processes were recorded. Optical texture observation was performed using a Nikon ECLIPSE E400 POL polarizing optical

microscope equipped with a Linkam THMS 600 heating and cooling stage. Purities of intermediates and final compounds were checked by HPLC analysis. Molecular weights of the polymers were determined by gel permeation chromatography (GPC) with a Shodex A-80M column and a JASCO HPLC 870-UV detector, with THF used as the solvent, with the instrument calibrated by polystyrene standard. XRD measurements were performed with a Rigaku D-3F diffractometer, in which X-ray power was set at 1200 mW. Molecular mechanics (MM) calculations for the polymers were carried out with a Silicon Graphics Cerius$^2$ software running on an Indigo$^2$ workstation.

*8-2.Chemicals*

PCH500 was purchased from Kanto chemical Ltd. Japan. (4-*trans*-4'-*n*-Alkylcyclohexyl)phenol was purchased from Kanto Chemical Japan. 4-(4'-Butyl-phenylazo)phenol (AB400) was prepared by an azo-coupling reaction between phenol and *p*-butyl aniline. THF, chloroform, and toluene were purified before use by distillation.

*8-3.Synthesis*

*8-3-1.* ***PCHR03A***

PCHR03A (R: methyl, propyl, pentyl, hexyl, heptyl, or octyl) was prepared by Williamson etherification with an aid of KI as a catalyst. Typical synthesis procedure of PCH703A is as follows. (4-*trans*-4'-*n*-heptylcyclohexyl)phenol (PCH700, 6.9 g, 25 mmol) was added to a solution of ethanol (25 mL) dissolving Na (0.7 g, 30 mmol) at rt. A solution of 5-chloro-1-pentyne (3 g, 30 mmol) in 25 mL ethanol was slowly added to the solution by pressure equalized dropping funnel. Then, catalytic amount of KI (0.1 g, 0.6 mmol) was added to the reaction mixture, and refluxed at

65 °C for 30 h. After evaporation, ether was added and the organic layer was washed with water several times. Then $CaCl_2$ was added. After removal of $CaCl_2$, ether was evaporated and the residue was recrystallized with ethanol. The white solid obtained was purified with column chromatography, where $CH_2Cl_2$ was used as an eluent. PCH703A was obtained in yield of 62 %. Anal. Calcd. for $C_{24}H_{36}O$: C, 84.65; H, 10.66. Found: C, 84.37; H, 10.72. IR (KBr, $cm^{-1}$): 3308 ($\nu_{HC\equiv}$), 2120 ($\nu_{C\equiv C}$), 628 ($\delta_{HC\equiv}$). $^{13}C$ NMR (125 MHz, δ from TMS, $CDCl_3$, ppm): 14.14, 15.24, 22.74, 27.06, 28.36, 29.43, 30.02, 31.97, 33.73, 34.65, 37.40, 37.50, 43.82, 66.16, 66.75 (H*C*≡C$CH_2$-), 83.61(HC≡*C*$CH_2$-), 114.35, 127.66, 140.27, 157.04. Transition temperatures: crystal (26 °C) nematic (33 °C) isotropic.

*8-3-2.* ***12-para-(trans-4'-pentyl-cyclohexyl)phenyl ester-1- dodecyne (PCH5CO10A)***

A solution of triphenylphosphine (TPP, 5.2 g, 20 mmol) and tridec-12-ynoic acid (3.8 g, 20 mmol) in 20 mL of THF was added to a solution of PCH500 (4.9 g, 20 mmol) and diethyl azodicarboxylate (DEAD, 40 % in toluene: 8.7 g, 20 mmol) in 10 mL of THF by pressure equalized dropping funnel under an argon atmosphere. After the reaction mixture was stirred for 24h at rt, the solution was evaporated, washed with water several times, and extracted by ether. After evaporation, the cure product was recrystallized from ethanol to afford 5.4 g of white powder (yield: 62 %). Anal. Calcd. for $C_{30}H_{46}$: C, 82.14; H, 10.57. Found: C, 82.18; H, 10.35. $^{13}C$ NMR (125 MHz, δ from TMS, $CDCl_3$, ppm): 14.12, 16.41, 22.75, 24.98, 25.65, 26.67, 28.48, 28.69, 28.94, 29.07, 29.15, 32.26, 33.63, 33.75, 34.42, 34.46, 37.35, 37.41, 44.13, 68.13 (H*C*≡C$CH_2$-), 84.64 (HC≡*C*$CH_2$-), 121.19 (ph), 128.57 (ph), 145.28 (ph), 148.75 (ph), 172.43 (*C*=O).

*8-3-3.* ***(4-Butyl-phenyl)-(4-pent-4-ynyloxy-benzylidene)-amine (AM403A)***

A solution of **3** (4.0 g, 21.3 mmol) and *4*-hydroxy aniline (3.2 g, 21.3 mmol) in 15 mL of absolute ethanol was refluxed at 60 °C for 24 h. The crude product was evaporated, and purified by recrystallization from ethanol to afford white powder (yield = 58 %). Anal. Calcd. for $C_{22}H_{25}N$: C, 82.72; H, 7.89; N, 4.38. Found: C, 82.69; H, 7.80; N, 4.12. $^{1}$H NMR (500 MHz, $CDCl_3$, δ from TMS, ppm): 0.80 (t, *J* = 7.0 Hz, 3H, $CH_3$), 1.24 (m, 2H, $CH_2$), 1.56 (m, 2H, $CH_2$) 1.91 (t, *J* = 2.7 Hz, 1H, *H*C≡), 1.96 (m, 2H, C*H*$_2$), 2.35 (m, *J* = 4.4 Hz, 2H, C*H*$_2$), 2.53 (t, *J* = 7.6 Hz, 2H, C*H*$_2$), 4.07 (t, *J* = 6.2 Hz, 2H, OC*H*$_2$), 6.69 (d, *J* = 6.9 Hz, 2H, ph), 6.92 (d, *J* = 8.2 Hz, 2H, ph), 7.10 (d, *J* = 5.0 Hz, 2H, ph), 7.75 (d, *J* = 5.0 Hz, 2H, ph), 8.30 (s, 1H, C*H*O). $^{13}$C NMR (125 MHz, δ from TMS, $CDCl_3$, ppm): 14.07 ($CH_3$), 15.07($CH_2$), 22.64 ($CH_2$), 28.07 ($CH_2$), 31.78 ($CH_2$), 35.06 ($CH_2$), 66.28 (O*C*H$_2$), 69.00 (H*C*≡C$CH_2$), 83.25 (HC≡*C*$CH_2$), 114.75 (ph), 120.73 (ph), 129.10 (ph), 130.38 (ph), 140.49 (ph), 158.83 (ph), 161.43 (*C*H=N).

*8-3-4.* ***(4-Butyl-phenyl)-(4-pent-4-ynyloxy-phenyl)-diazene (AB403A)***

This compound was prepared using a method similar to that described for PCHR03A. Quantity used: AB400 (2 g, 8 mmol), Na (0.18 g, 8 mmol), KI (0.5 g, 3 mmol), 5-chloro-1-pentyne (1 g, 9.6 mmol), and ethanol (5 mL). The crude compound was purified by recrystallization from ethanol to yield gold colored crystal (yield: 0.74 g, 29 %). Anal. Calcd. for $C_{21}H_{24}N_2$: C, 78.76; H, 7.50; N, 8.74. Found: C, 78.43; H, 7.53; N, 8.76. IR (KBr, $cm^{-1}$): 3323 ($\nu_{HC\equiv}$), 2120 ($\nu_{C\equiv C}$), 623, 607 ($\delta_{HC\equiv}$). $^{1}$H NMR (500 MHz, $CDCl_3$, δ from TMS, ppm): 0.94 (t, *J* = 7.4 Hz, 3H, ph-$CH_2CH_2CH_2CH_3$), 1.37 (sextet, *J* = 7.5 Hz, 2H, ph-$CH_2CH_2CH_2CH_3$), 1.63 (quint, *J* = 7.7 Hz, 2H, ph-$CH_2CH_2CH_2CH_3$),

1.99 (t, *J* = 2.5 Hz, 1H, HC≡), 2.05 (quint, *J* = 6.5 Hz, 2H, HC≡CCH$_2$C*H$_2$*CH$_2$O-), 2.43 (m, 2H, HC≡CC*H$_2$*CH$_2$CH$_2$O-), 2.67 (t, 2H, *J* = 7.8 Hz, ph-C*H$_2$*CH$_2$CH$_2$CH$_3$), 4.15 (d, *J* = 6.2 Hz, 2H, HC≡CCH$_2$CH$_2$C*H$_2$*O-), 6.99 (d, *J* = 8.9 Hz, 2H, ph), 7.29 (d, *J* = 8.3 Hz, 2H, ph), 7.79 (d, *J* = 8.3, 2H, ph), 7.90 Hz (d, *J* = 8.8 Hz, 2H, ph). $^{13}$C NMR (125 MHz, δ from TMS, $CDCl_3$, ppm): 13.93, 15.17, 22.34, 28.12, 33.48, 35.56, 66.46 (O*C*H$_2$), 69.02 (H*C*≡CCH$_2$), 83.29 (HC≡*C*CH$_2$), 114.72, 122.54, 124.57, 129.05, 145.82, 147.16, 151.07, 161.17. Transition temperatures: crystal (43 °C) nematic (47 °C) isotropic.

Synthetic procedure, elemental analysis, IR, and NMR data of other compounds were described in supplementary data.

**Acknowledgements**

We would like to thank Professor Hideki Shirakawa of University of Tsukuba for valuable discussions and advice. The authors also thank Messrs. J. Murakami, Y. Bannai, and H. Yoneyama for their assistance. This work was supported by a Grant-in-Aid for Science Research in a Priority Area "Super-Hierarchical Structures" from the Ministry of Education, Culture, Sports, Science and Technology, Japan.

**References**

[1] K. Akagi, S. Katayama, H. Shirakawa, K. Araya, A. Mukoh and T. Narahara, Synth. Met. 17

(1987) 241.

[2] (a) H. Shirakawa, S. Fukumoto, H. Tanaka, Y. Ugawa and K. Akagi, J. Macromol. Sci. Chem. 11-12 (1991) 1245. (b) K. Yoshino, K. Kobayashi, K. Myojin, M. Ozaki, K. Akagi, H. Goto and H. Shirakawa, Jpn. J. Appl. Phys. 35 (1996) 3964. (c) B.Z. Tang, X.X. Kong and X.D. Feng, Chinese J. Polym. Sci., Part A: Polym. Chem. Ed. 17 (1999) 289. (d) X. Kong and B.Z. Tang, Chem. Mat. 10 (1998) 3352. (e) J.W.Y Lam, Y. Dong, K.K.L. Cheuk, J. Luo, Z. Xie, H.S. Kwok, Z. Mo and B.Z. Tang, Macromolecules 35 (2002) 1229. (f) P. Stagnaro, B. Cavazza, V. Trefiletti, G. Costa, B. Gallot and B. Valenti, Macromol. Chem. Phys. 202 (2001) 2065. (g) J. Le Moigne, A. Hilberer, F. Kajzar and A. Thierry, NATO ASI Series E: Appl. Sci. 194 (1991) 327. (h) S. Koltzenburg, F. Stelzer and O. Nuyken, Macromol. Chem. Phys. 200 (1999) 821. (i) S. Koltzenburg, D. Wolff and F. Stelzer, Macromolecules 31 (1998) 9166. (j) S. Koltzenburg, F. Stelzer and O. Nuyken, Macromol. Chem. Phys. 200 (1999) 821. (k) W.Y. Lam, X. Kong, B.Z. Tang, Polym. Mat. Sci. Eng. 80 (1999) 159. (l) K. Akagi and H. Shirakawa, Curr. Trends Polym. Sci. 2 (1997) 107. (m) J.X. Geng, E.L. Zhou, G. Li, J.W.Y. Lam and B.Z. Tang, J. Polym. Sci., Part B: Polym. Phys. 42 (2004) 1333. (n) S.Y. Oh, K. Akagi and H. Shirakawa, Hwahak Konghak 34 (1996) 154. (o) S.Y. Oh, K. Akagi and H. Shirakawa, Hwahak Konghak 34 (1996) 70. (p) S.Y. Oh, R. Ezaki, K. Akagi and H Shirakawa, J. Polym. Sci., Part A: Polym. Chem. Ed. 31 (1993) 2977. (q) S.Y. Oh, K. Akagi, H. Shirakawa and K. Araya, Macromolecules 26 (1993) 6203. (r) C. Ye, G. Xu, Z.Q. Yu, J.W.Y. Lam, J.H. Jang, H.L. Peng, Y.F. Tu, Z.F. Liu, K.U. Jeong, S.Z.D. Cheng, E.Q. Chen and B.Z. Tang, J. Am. Chem. Soc. 127

(2005) 7668. (s) Goto and H. Akagi, K., J. Polym. Sci., Part A: Polym. Chem. Ed. 43 (2005) 616. (t) H. Goto, X-M. Dai, T. Ueoka and K. Akagi, Macromolecules 37 (2004) 4783. (u) H. Goto, X-M. Dai, H. Narihiro and K. Akagi, Macromolecules 37 (2004) 2353.

[3] (a) R.H.L. Kiebooms, H. Goto and K. Akagi, Macromolecules 34 (2001) 7989. (b) G. Piao, H. Goto, K. Akagi and H Shirakawa, Polymer 39 (1998) 3559.

[4] (a) C.I. Simionescu, V. Percec and S. Dumitorescu, J. Polym. Sci., Part A: Polym. Chem. Ed. 15 (1977) 2497. (b) M. Tabata, S. Kobayashi, Y. Sadahiro, Y. Nozaki, K. Yokota and W. Yang, J. Macromol. Sci. Pure Appl. Chem. A34 (1997) 641.

(c) M. Tabata, Y. Sadahiro, K. Yokota and S. Kobayashi, Jpn. J. Appl. Phys., Part 1: Regular Papers, Short Notes Rev. Papers 35 (1996) 5411. (d) H. Minakawa, M. Tabata and K. Yokota, J. Macromol. Sci. Pure Appl. Chem. A33 (1996) 291. (e) K. Akagi and H. Shirakawa, Macromol. Symp. 104 (1996) 137.

[5] (a) H. Finkelmann, H. Ringsdorf and J.H. Wendorf, Makromol. Chem. 179 (1978) 273. (b) H. Finkelmann, H. Ringsdorf, W. Siol and J.H. Wendorf, ACS Symp. Ser. 74 (1978) 22. (c) V.P. Shivaev, N.A. Platé and Y.S. Friedson, J. Polym. Sci., Part A: Polym. Chem. Ed. 17 (1979) 1655. (d) V.P. Shivaev and N.A. Platé, Polymer 24 (1983) 364. (e) H. Finkelmann and G. Rehage, Makromol. Chem. Rapid Commun. 1 (1980) 31.

[6] J.J. Wysocki, J. Adams and W. Haas, Phys. Rev. Lett. 20 (1968) 1024.

[7] K. Iino, H. Goto, K. Akagi, H. Shirakawa and A. Kawaguchi, Synth. Met. 84 (1997) 967.

[8] Y. Kuwae, T. Masuda and T. Higashimura, Polym. J. (Tokyo) 12 (1980) 387.

[9] S.Y. Oh, S.M. Hong and S.I. Oh, Mol. Cryst. Liq. Cryst. 295 (1997) 105.

[10] M. Teraguchi and T. Masuda, Macromolecules 33 (2000) 240.

[11] S. Yin, H. Xu, W. Shi, Y. Gao, Y. Song, J. Wing, Y. Lam, B.Z. Tang, Polymer 46 (2005) 7670.

[12] (a) A. Izumi, R. Nomura and T. Masuda, Macromolecules 34 (2001) 4342. (b) J.J. Delang, J.M. Robertson and I. Woodward, Proc. Royal Soc. London, Ser. A, 171 (1939) 398.

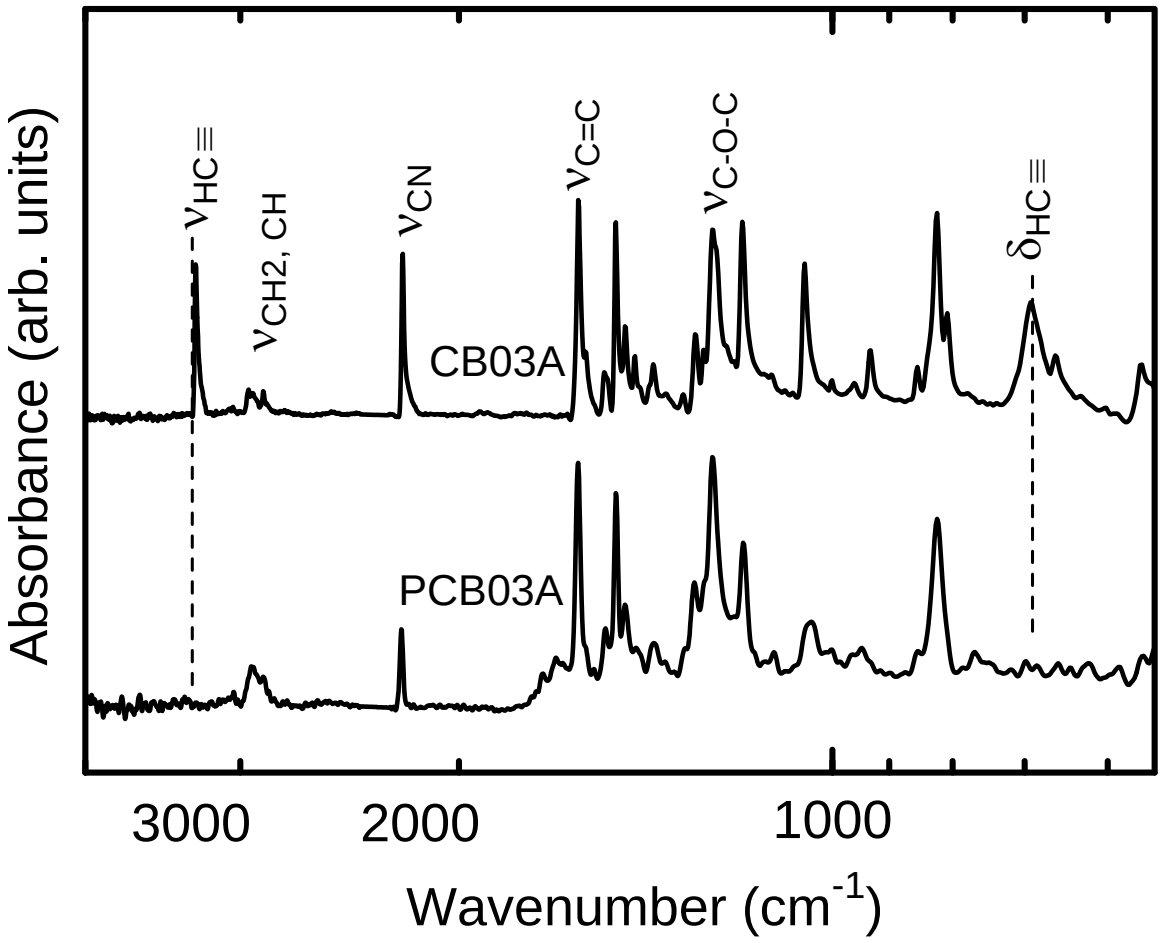


**Figure 1.** IR spectra of CB03A monomer (upper) and PCB03A(Rh) polymer (lower).

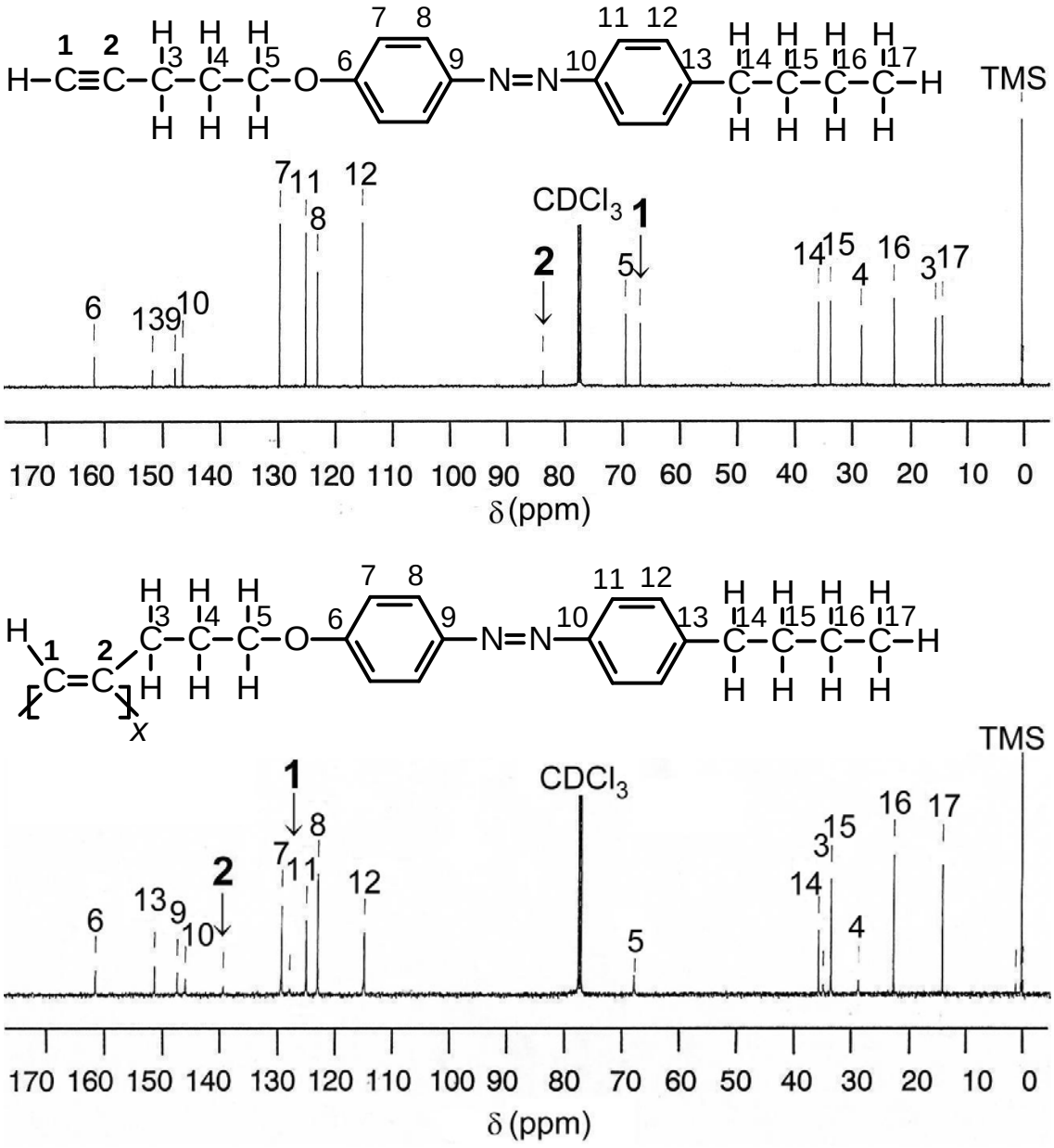


**Figure 2.** $^{1}$H NMR spectra of AB403A monomer (upper) and PAB403A(Rh) polymer (lower).

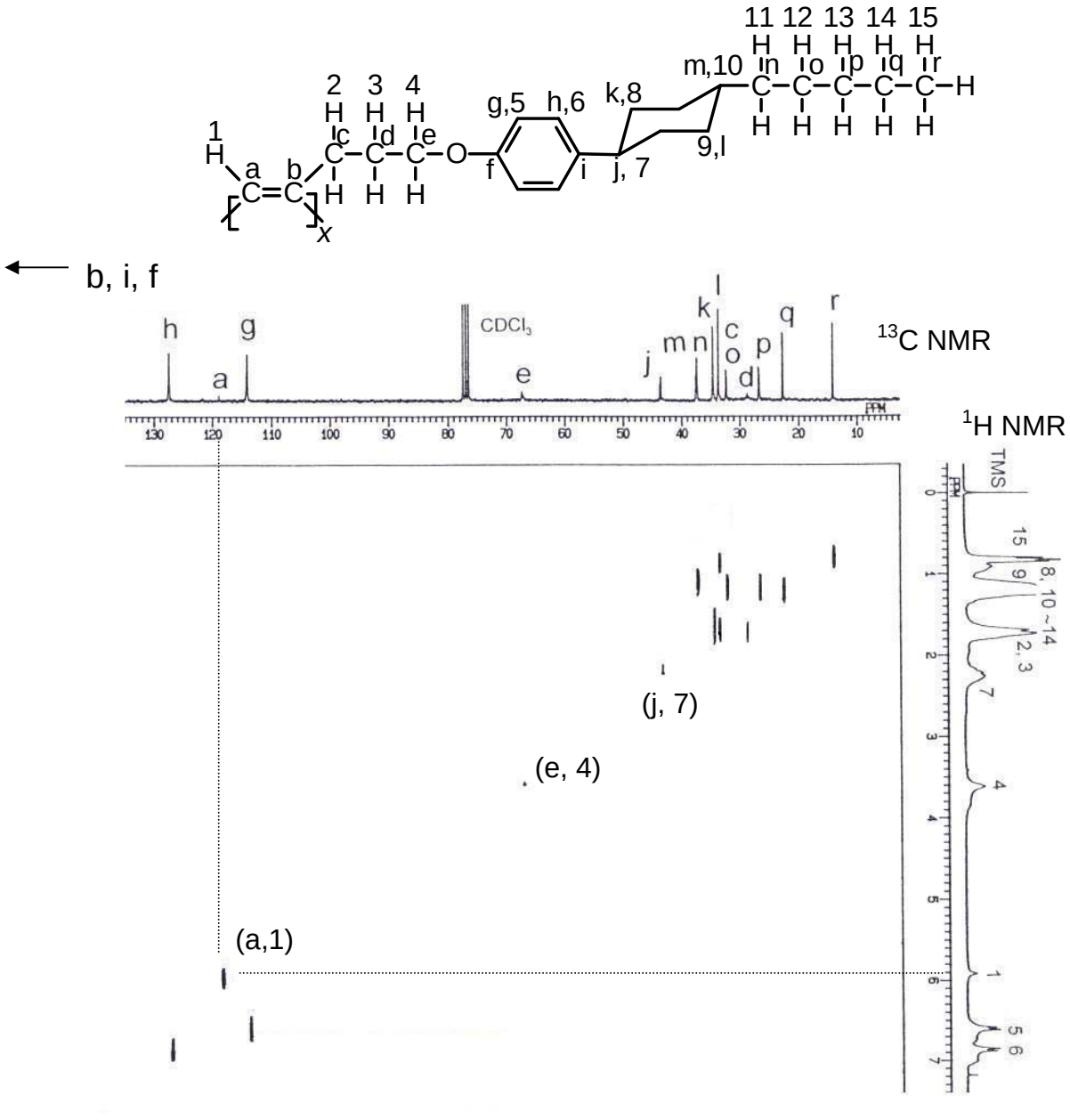


**Figure 3.** $^{13}C$–$^{1}H$ COSY NMR of PPCH503A (Rh) polymer.

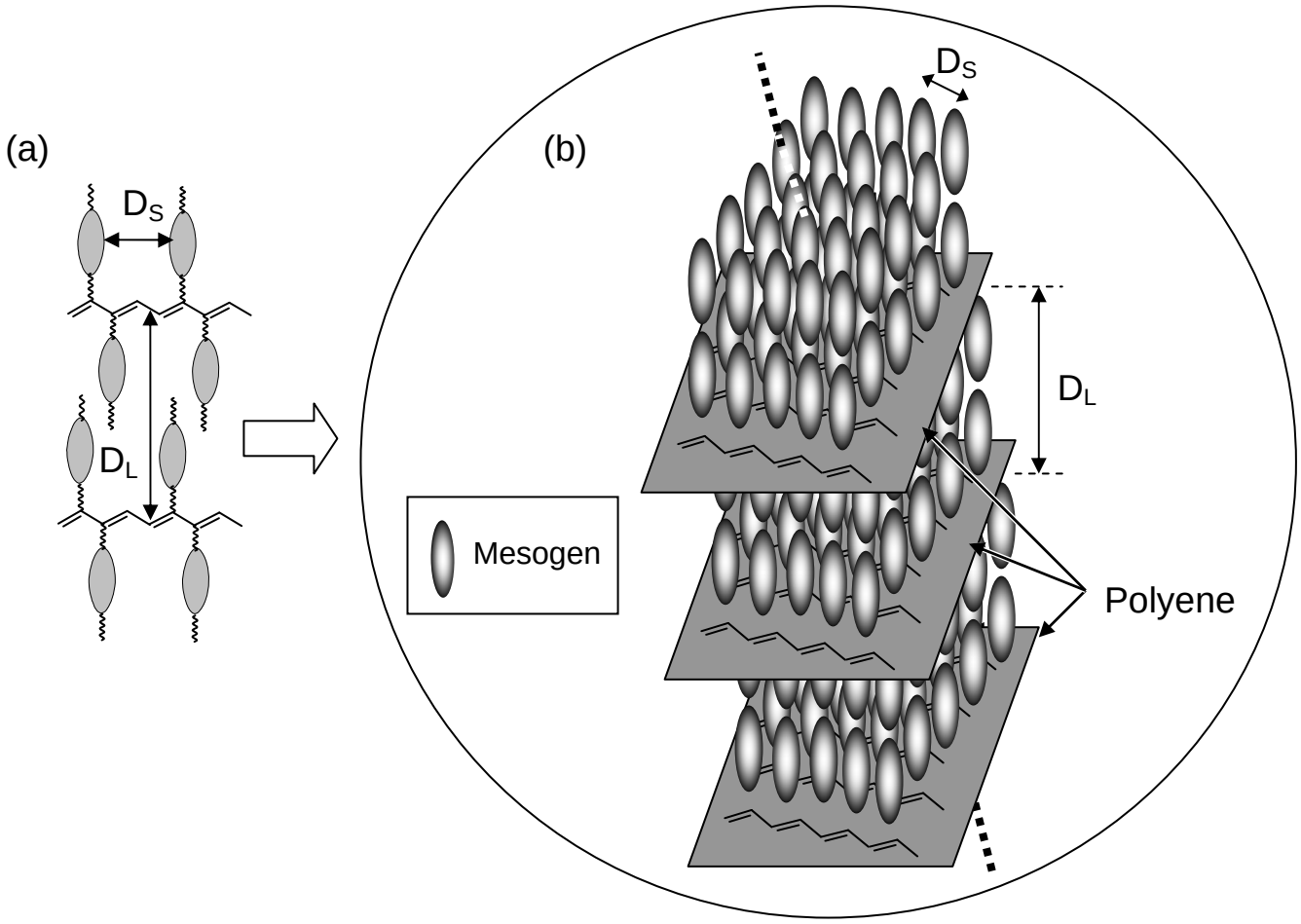


**Figure 4.** Molecular structure of polymer in smectic LC state: (a) layer structure, (b) plausible polymer structure. Inter-side-chain distances between LC molecules and inter-layer distances of the polymer are denoted $D_S$ and $D_L$. Flexible alkyl spacers and terminal alkyl groups of the side-chain LC group are omitted in (b).

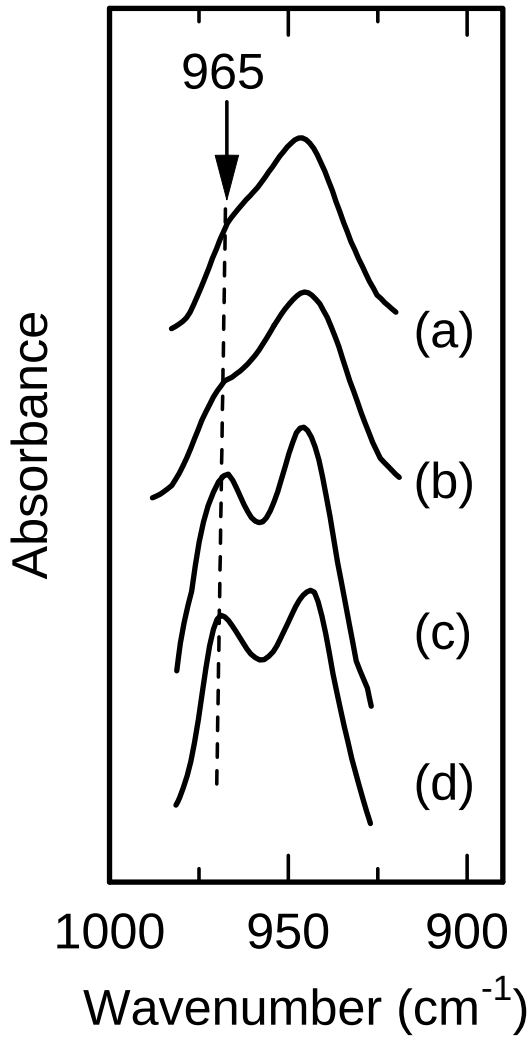


**Figure 5.** IR spectra of PPCH503A(Rh) polymer after heating for 10 min in argon: (a) 80, (b) 120, (c) 160, and (d) 200 °C.

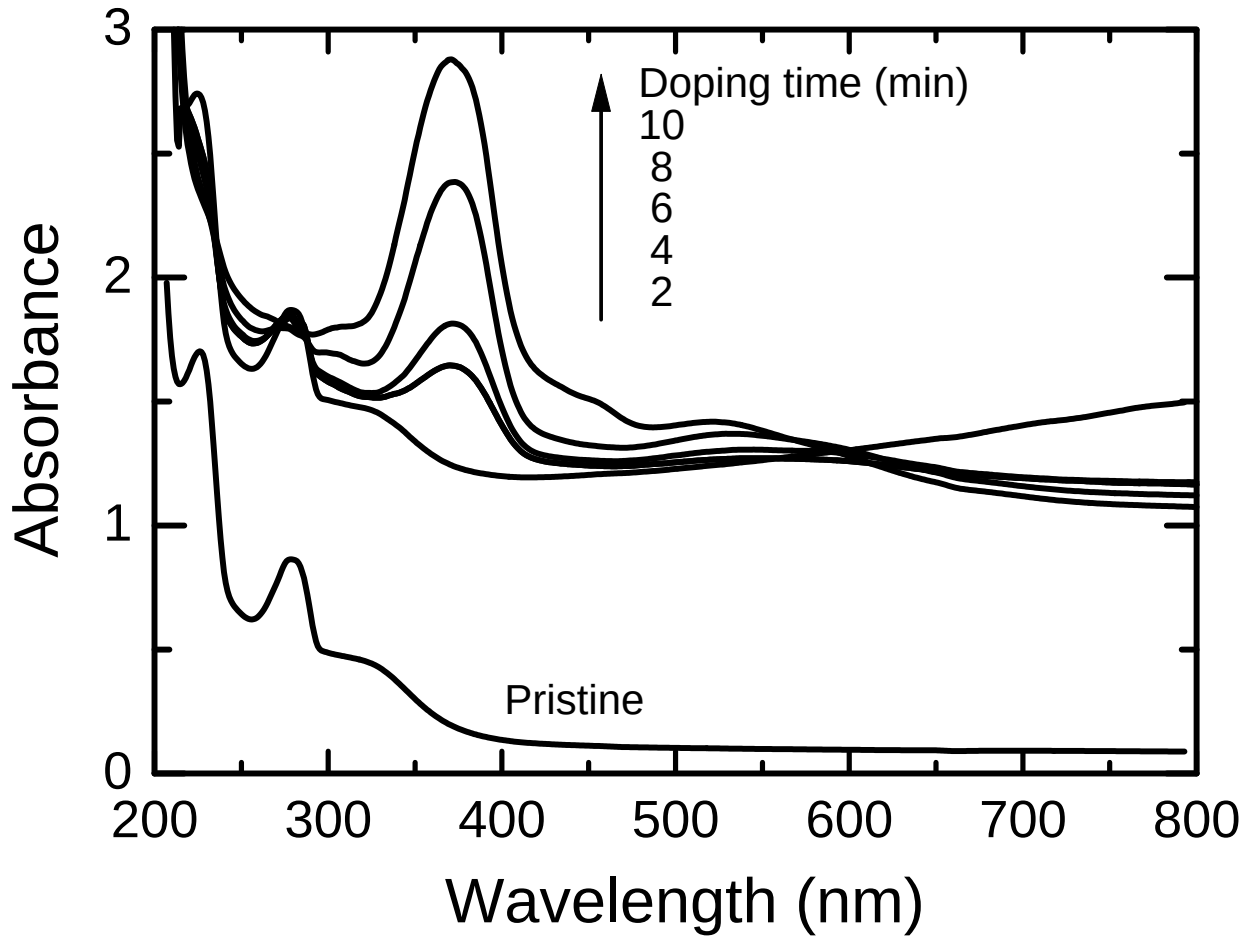


**Figure 6.** *In-situ* UV-vis absorption spectra of PPCH503A(Rh) polymer doped with $AsF_5$ in the gas phase.

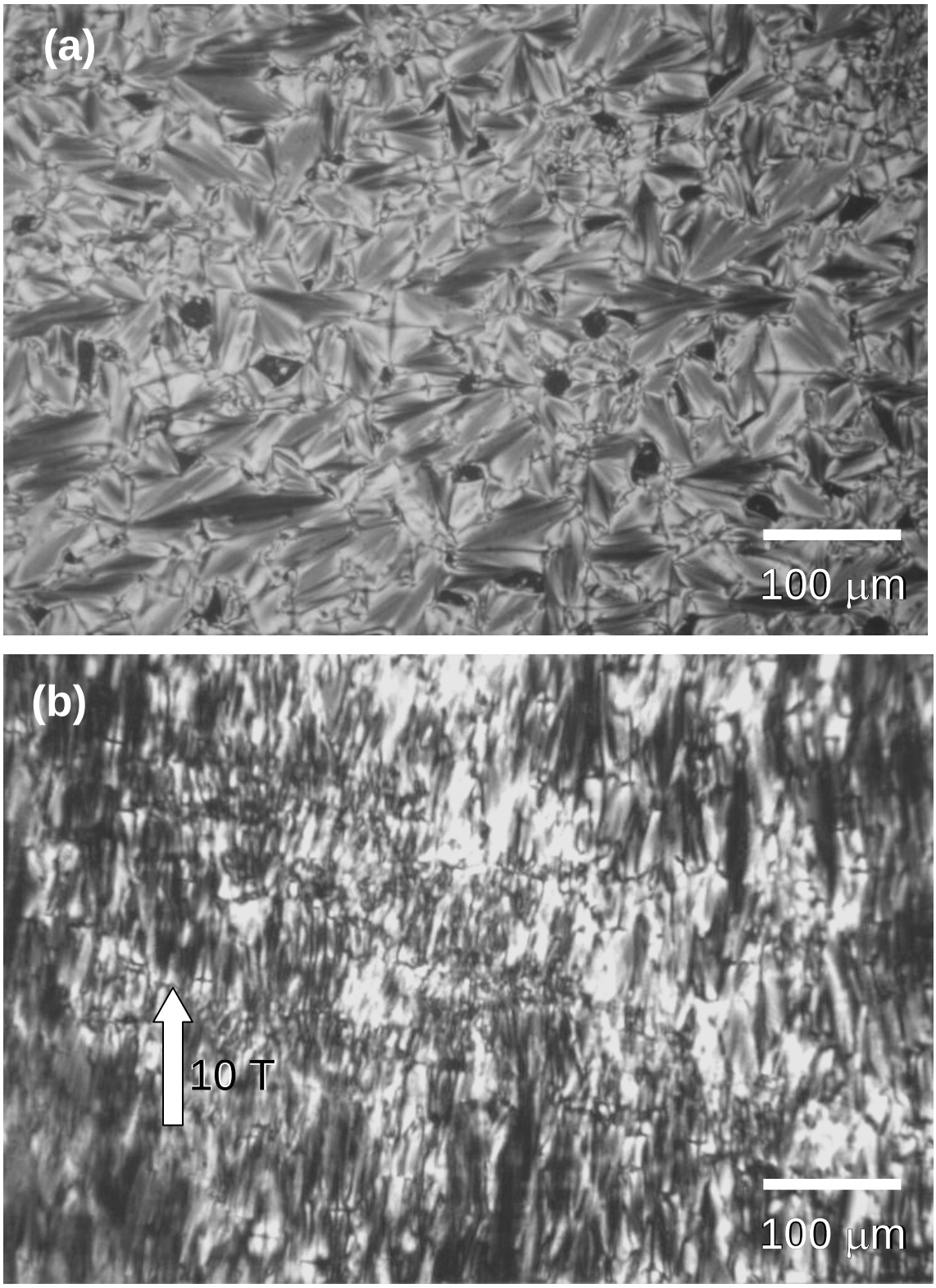


**Figure 7.** POM images of PPCH503A(Rh) (a) before and (b) after application of an external magnetic field (10 Tesla).

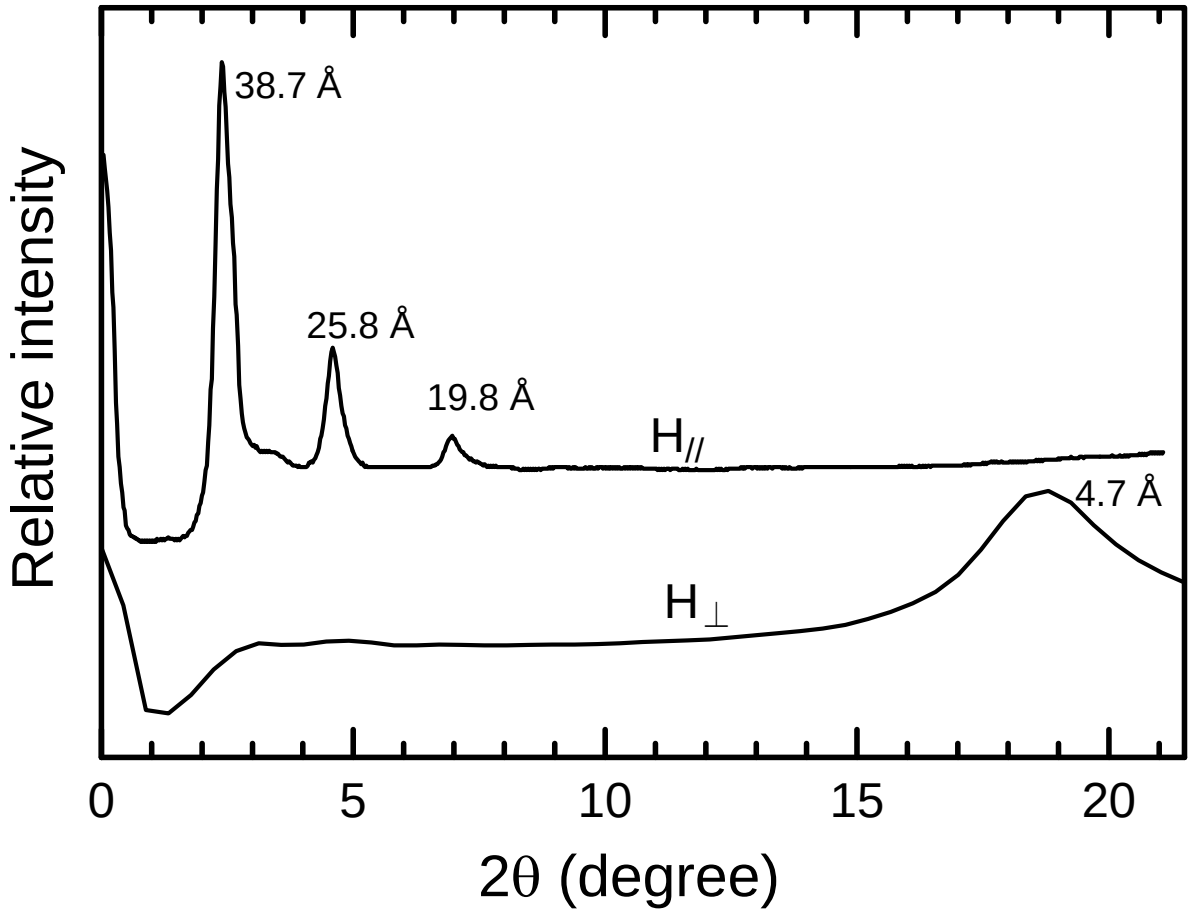


**Figure 8.** XRD patterns of PPCH503A(Rh) polymer after application of an external magnetic field (10 Tesla). $H_{//}$ and $H_{\perp}$ denote directions parallel and perpendicular to the magnetic field vector.

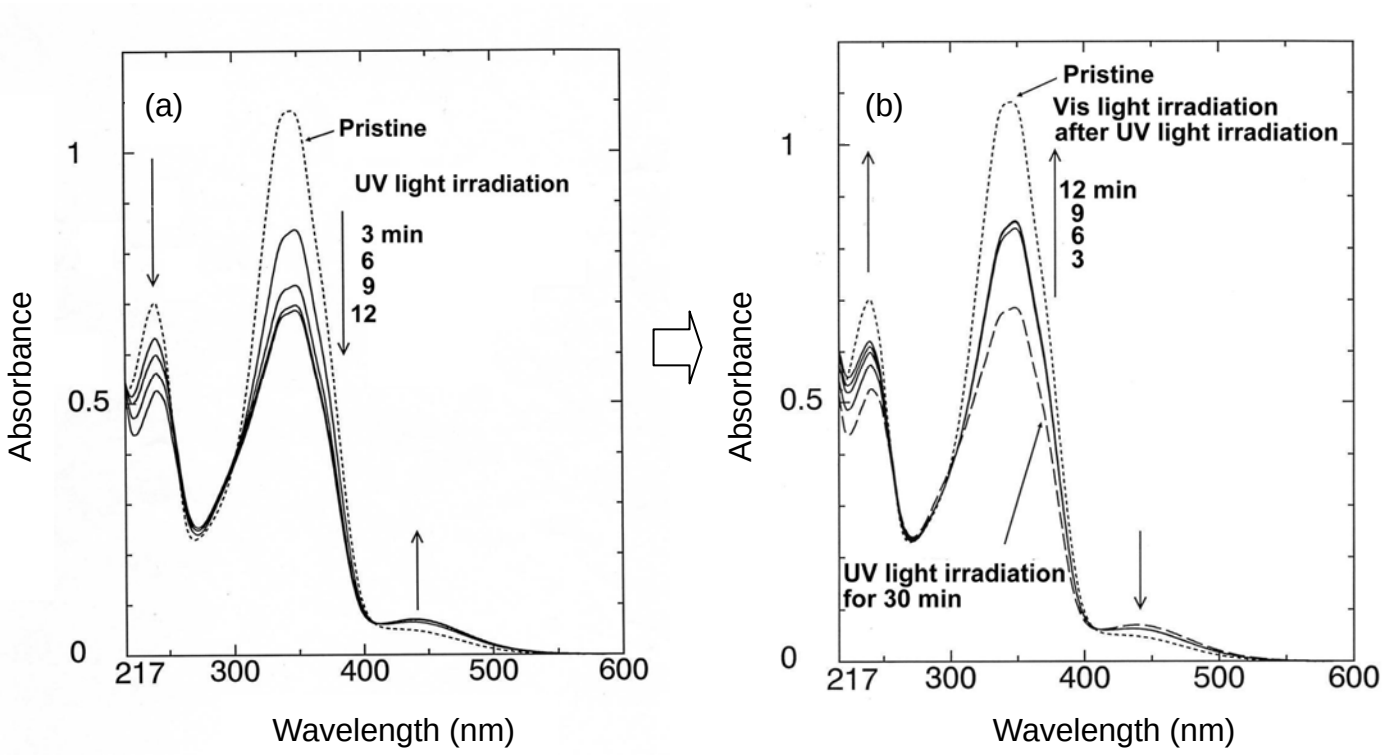


**Figure 9.** UV-vis absorption spectra of PAB403A(Rh) polymer (a) upon UV irradiation (<300 nm) in THF, and (b) upon subsequent visible-light irradiation (>450 nm) in THF.

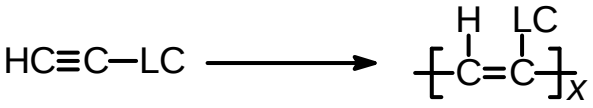

| Polymer | LC (mesogenic group) | | Catalyst-cocatalyst |
|---|---|---|---|
| PPCH203A (Mo) | 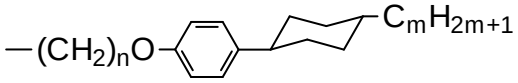 | n = 3, m = 2 | $MoCl_5$-$Ph_4Sn$ |
| PPCH303A (Mo) | | n = 3, m = 3 | $MoCl_5$-$Ph_4Sn$ |
| PPCH503A (Mo) | | n = 3, m = 5 | $MoCl_5$-$Ph_4Sn$ |
| PPCH603A (Mo) | | n = 3, m = 6 | $MoCl_5$-$Ph_4Sn$ |
| PPCH703A (Mo) | | n = 3, m = 7 | $MoCl_5$-$Ph_4Sn$ |
| PPCH803A (Mo) | | n = 3, m = 8 | $MoCl_5$-$Ph_4Sn$ |
| PPCH803A (Fe) | | n = 3, m = 8 | $Fe(acac)_3$-$Et_3Al$ |
| PPCH503A (Rh) | | n = 3, m = 5 | $[Rh(NBD)Cl]_2$-$Et_3N$ |
| PPCH506A (Rh) | | n = 6, m = 5 | $[Rh(NBD)Cl]_2$-$Et_3N$ |
| PPCH506A (Fe) | | n = 6, m = 5 | $Fe(acac)_3$-$Et_3Al$ |
| PPCH506A (Mo) | | n = 6, m = 5 | $MoCl_5$-$Ph_4Sn$ |
| PPCH5010A (Rh) | | n = 10, m = 5 | $[Rh(NBD)Cl]_2$-$Et_3N$ |
| PPCH5C010A (Rh) | 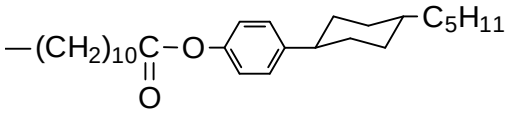 | | $[Rh(NBD)Cl]_2$-$Et_3N$ |
| PBP503A (Rh) | 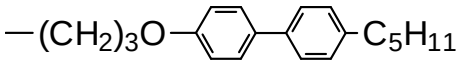 | | $[Rh(NBD)Cl]_2$-$Et_3N$ |
| PCB03A (Rh) | 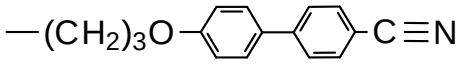 | | $[Rh(NBD)Cl]_2$-$Et_3N$ |
| PCB03A (Fe) | | | $Fe(acac)_3$-$Me_2S{\cdot}BH_3$ |
| PAM403A (Fe) | 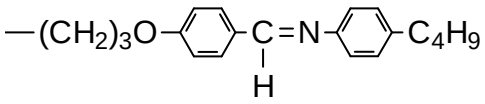 | | $Fe(acac)_3$-$Et_3Al$ |
| PAB403A (Rh) | 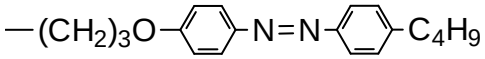 | | $[Rh(NBD)Cl]_2$-$Et_3N$ |
| PAB403A (Fe) | | | $Fe(acac)_3$-$Et_3Al$ |

**Scheme 7.**

**Table 1.** Polymerization results of PCH503A.

| Entry | [M]/[cat][a] | $M_n$[b] | $M_w$[c] | MWD[d] | Yield (%) |
|---|---|---|---|---|---|
| Run 1 | 10 | 27200 | 46200 | 1.7 | 60 |
| Run 2 | 100 | 28000 | 71000 | 2.5 | 39 |
| Run 3 | 1000 | 33700 | 77500 | 2.3 | 10 |
| Run 4 | 1500 | 26500 | 58300 | 2.2 | 5 |

[a]M: monomer, cat: catalyst. [b]number-average molecular weight evaluated relative to a polystyrene (PS) standard. [c]weight-average molecular weight evaluated relative to PS standard. [d]Molecular weight distribution relative to PS standard.

**Table 2.** Polymerization results, transition temperatures, and *cis-trans* isomerization temperatures of main-chain.

| Polymer | $M_n$[b] (x $10^4$) | $M_w$[b] (x $10^4$) | MWD[b] | Yield (%) | *Cis* proton[c] (ppm) | Transition temperature (°C)[d] | *Cis-trans*[e] (°C) |
|---|---|---|---|---|---|---|---|
| PPCH203A (Mo) | 6.7 | 15.8 | 2.4 | 77 | — | Mp ~ 91 (no LC) | — |
| PPCH303A (Mo) | 1.5 | 3.4 | 2.3 | 62 | — | G·110·Sm·133·I | — |
| PPCH503A (Mo) | 1.4 | 3.3 | 2.4 | 67 | — | G·86·Sm·171·I | — |
| PPCH603A (Mo) | 3.3 | 5.7 | 1.7 | 68 | — | G·52m·180·I | — |
| PPCH703A (Mo) | 1.5 | 4.2 | 2.8 | 70 | — | G·71·Sm·135·I | — |
| PPCH803A (Mo) | 1.2 | 2.7 | 2.3 | 73 | — | G·132·Sm·189·I | — |
| PPCH803A (Fe) | 52 | 260 | 5.0 | 67 | 5.97 | G·77·Sm·150·I | 191 |
| PPCH503A (Rh) | 2.8 | 7.1 | 2.5 | 39 | 5.98 | G·69·Sm·142·I | 172 |
| PPCH506A (Rh) | 1.6 | 2.5 | 1.6 | 72 | 5.98 | G·70·Sm·125·I | 175 |
| PPCH506A (Fe) | 33.0 | 82.0 | 2.5 | 32 | 5.83 | G·67·Sm·140·I | 185 |
| PPCH506A (Mo) | 5.9 | 8.4 | 1.4 | 48 | — | G·83·Sm·130·I | — |
| PPCH5010A (Rh) | 1.2 | 3.3 | 2.8 | 31 | — | G·61·Sm·91·I | — |
| PBP50C010A (Rh) | 1.5 | 3.2 | 2.1 | 35 | 5.98 | G·78·Sm·109·I | 188 |
| PBP503A (Rh) | 3.0 | 6.1 | 2.0 | 70 | 5.95 | G·126·Sm·188·I | 189 |
| PCB03A (Rh) | 1.7 | 9.3 | 5.6 | 75 | 5.92 | G·67·Sm·131·I | 188 |
| PCB03A (Fe) | 0.4 | 0.6 | 1.5 | 83 | — | Mp > 200 (no LC) | 188 |
| PAM403A (Fe) | —[f] | —[f] | —[f] | 87 | —[f] | G·69·Sm·166·I | 201 |
| PAB403A (Rh) | 9.6 | 30.0 | 3.2 | 92 | 5.98 | G·88·Sm·165·I | 189 |
| PAB403A (Fe) | 12.0 | 41.0 | 3.4 | 88 | 5.95 | G·107·Sm·181·I | 192 |

[a][Mon]/[cat] = 100. [b]Polystyrene standard. [c]Signal of olefin proton of *cis* form in $^1$H NMR. [d]first cooling process. Transition temperatures were determined by DSC and polarizing optical microscopy observations. [e]*Cis-trans* isomerization exothermic trough determined by first heating process on DSC. [f]insoluble in $CDCl_3$.

**Figure captions**

**Figure 1.** IR spectra of CB03A monomer (upper) and PCB03A(Rh) polymer (lower).

**Figure 2.** $^{1}$H NMR spectra of AB403A monomer (upper) and PAB403A(Rh) polymer (lower).

**Figure 3.** $^{13}$C–$^{1}$H COSY NMR of PPCH503A (Rh) polymer.

**Figure 4.** Molecular structure of polymer in smectic LC state: (a) layer structure, (b) plausible polymer structure. Inter-side-chain distances between LC molecules and inter-layer distances of the polymer are denoted $D_S$ and $D_L$. Flexible alkyl spacers and terminal alkyl groups of the side-chain LC group are omitted in (b).

**Figure 5.** IR spectra of PPCH503A(Rh) polymer after heating for 10 min in argon: (a) 80, (b) 120, (c) 160, and (d) 200 °C.

**Figure 6.** *In-situ* UV-vis absorption spectra of PPCH503A(Rh) polymer doped with $AsF_5$ in the gas phase.

**Figure 7.** POM images of PPCH503A(Rh) (a) before and (b) after application of an external magnetic field (10 Tesla).

**Figure 8.** XRD patterns of PPCH503A(Rh) polymer after application of an external magnetic field (10 Tesla). $H_{//}$ and $H_{\perp}$ denote directions parallel and perpendicular to the magnetic field vector.

**Figure 9.** UV-vis absorption spectra of PAB403A(Rh) polymer (a) upon UV irradiation (<300 nm) in THF, and (b) upon subsequent visible-light irradiation (>450 nm) in THF.

**Table 1.** Polymerization results of PCH503A.

**Table 2.** Polymerization results, transition temperatures, and *cis-trans* isomerization temperatures of main-chain.

# Supplementary data for :

## Synthesis and Properties of Mono-Substituted Liquid Crystalline Polyacetylene Derivatives – Doping, Magnetic Orientation, and Photo-isomerization

Hiromasa Goto[a], Shigeki Nimori[b], Kazuo Akagi*,[a]

[a]Tsukuba Research Center for Interdisciplinary Materials Science (TIMS), Institute of Materials Science, University of Tsukuba, Tsukuba, Ibaraki 305-8573, Japan.

[b]Tsukuba Magnet Laboratory, National Research Institute for Metals, Tsukuba, Ibaraki 305-0003, Japan

*Correspondence to: K. Akagi, *e-mail*: akagi@ims.tsukuba.ac.jp

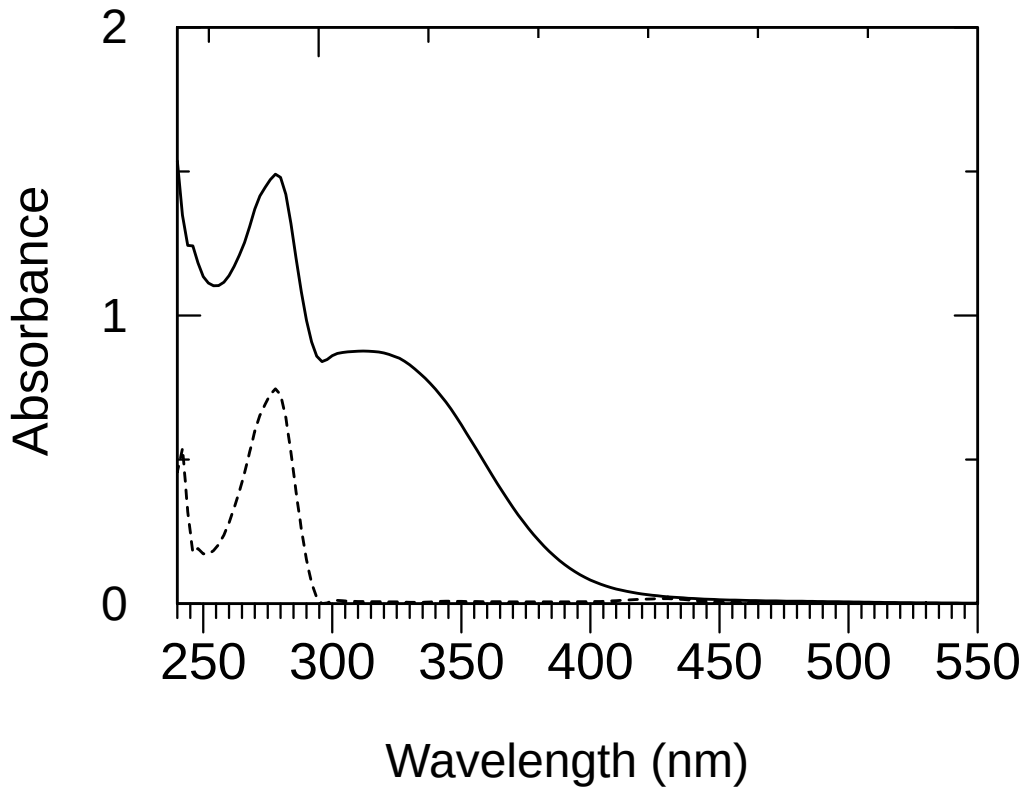


**Figure S1.** UV-vis absorption spectra for PCH503A monomer (dashed line) and PPCH503A(Rh) polymer (solid line) in THF solution.

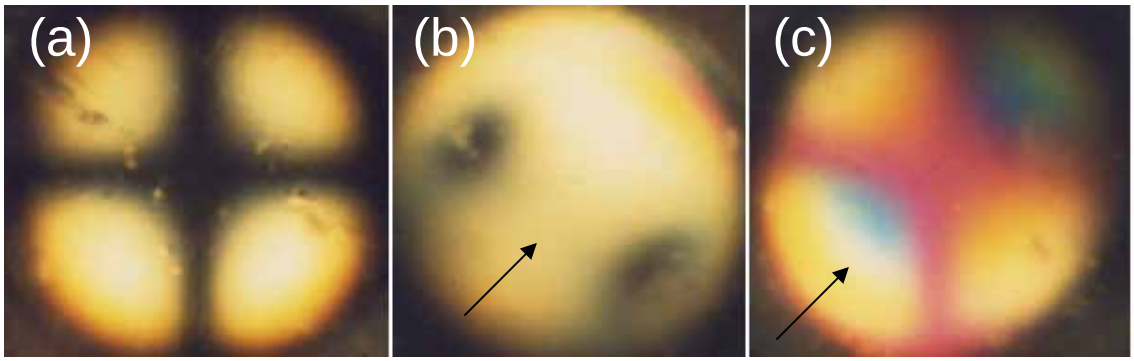


**Figure S2.** Conoscope patterns of perpendicular-oriented part of PPCH503A(Rh) polymer, showing (a) a Maltese cross, (b) insertion of 1/4 wavelength plate, and (c) insertion of gypsum first-order red plate. Arrows indicate insertion direction of the plates.

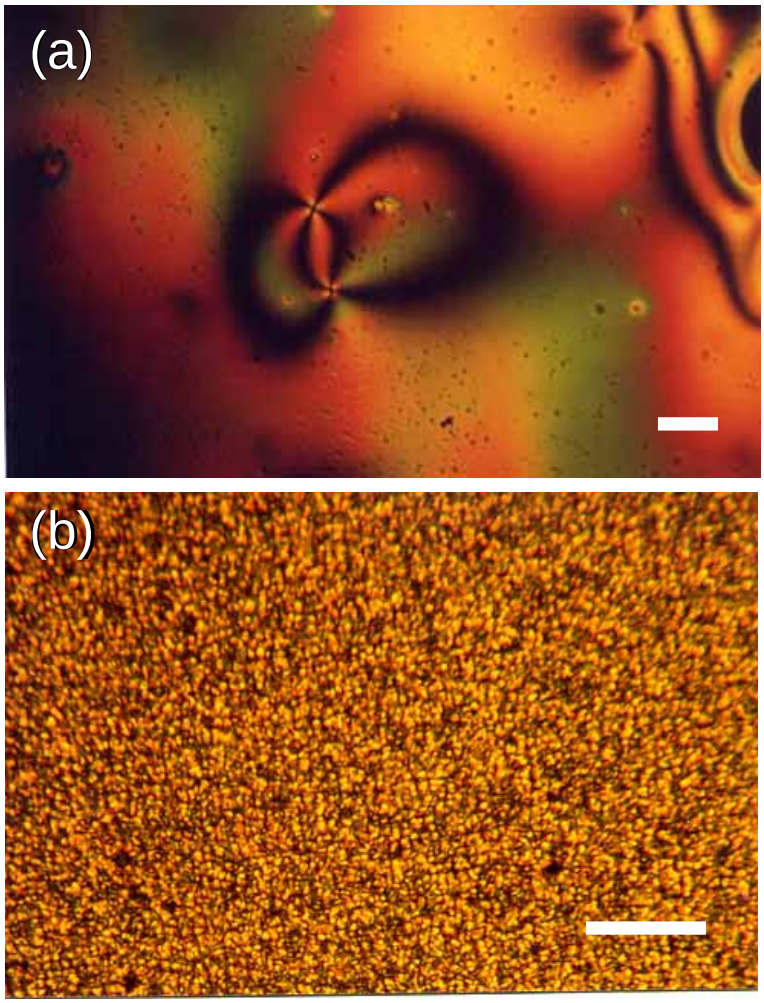


**Figure S3.** POM images of AB403A monomer (upper) at 45 °C and PAB403A(Rh) polymer (lower) at 80 °C (scale bar: 50 μm)

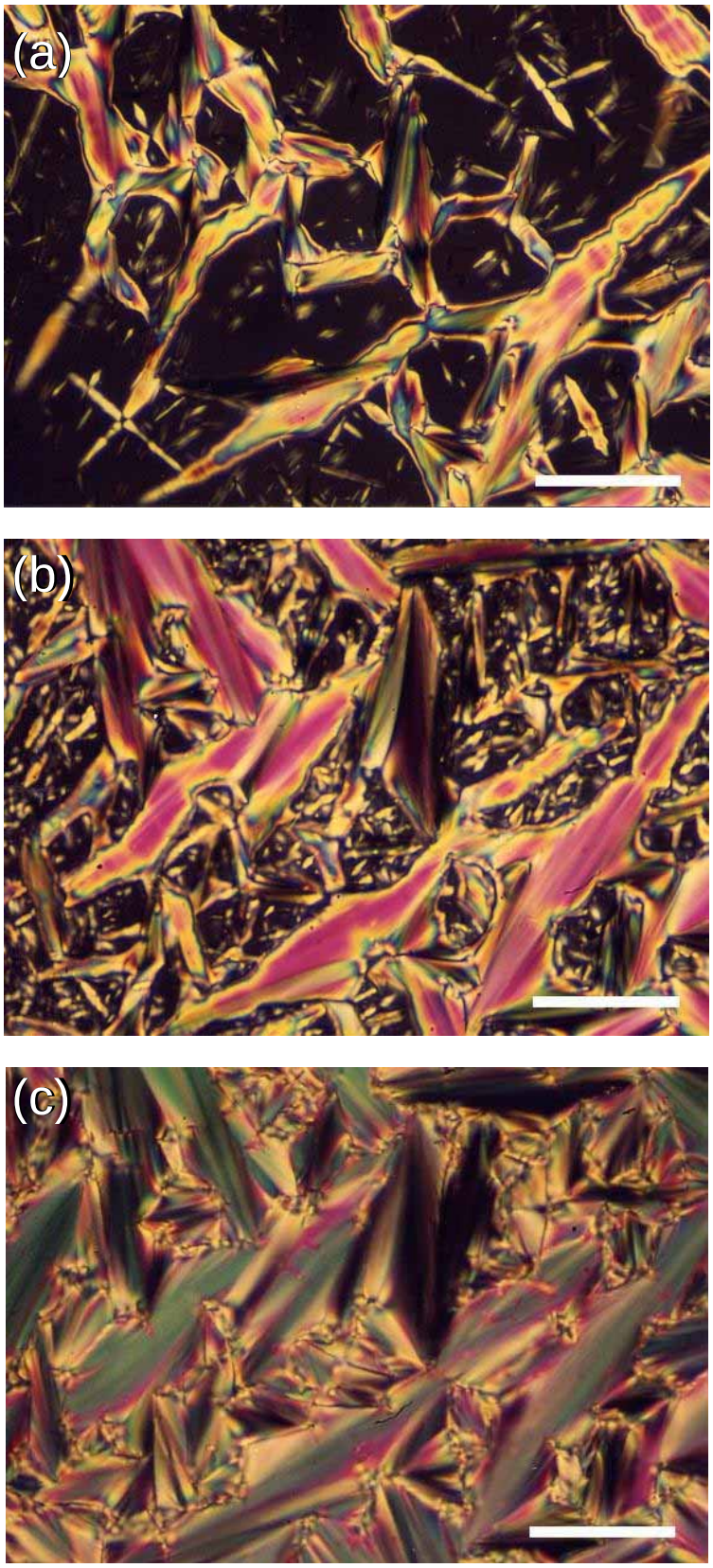


**Figure S4.** POM images of PPCH803A(Mo) polymer during cooling: (a) 172, (b) 162, and (c) 136 °C (scale bar: 100 μm).

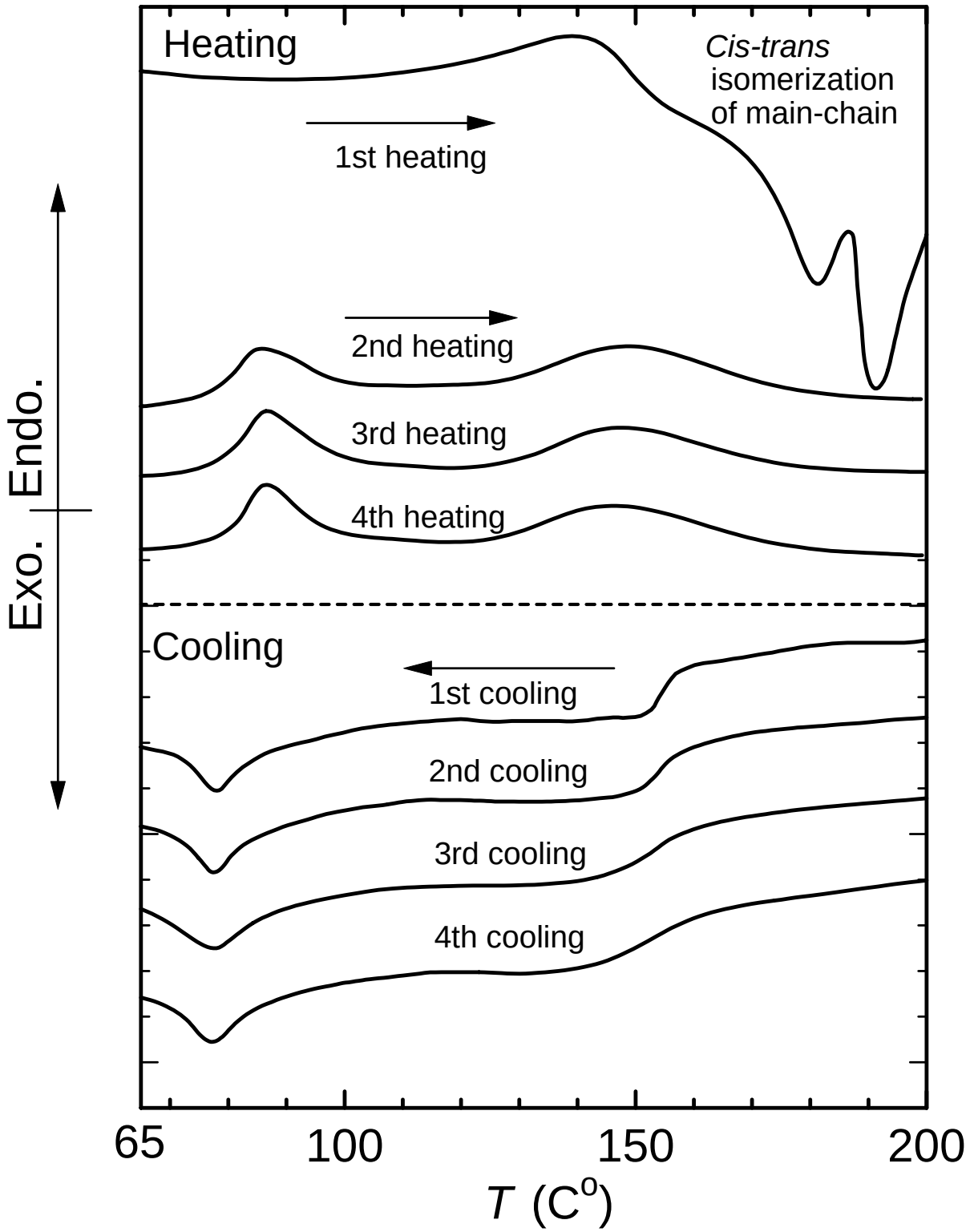


**Figure S5.** DSC curves of PPCH803A(Fe) polymer.

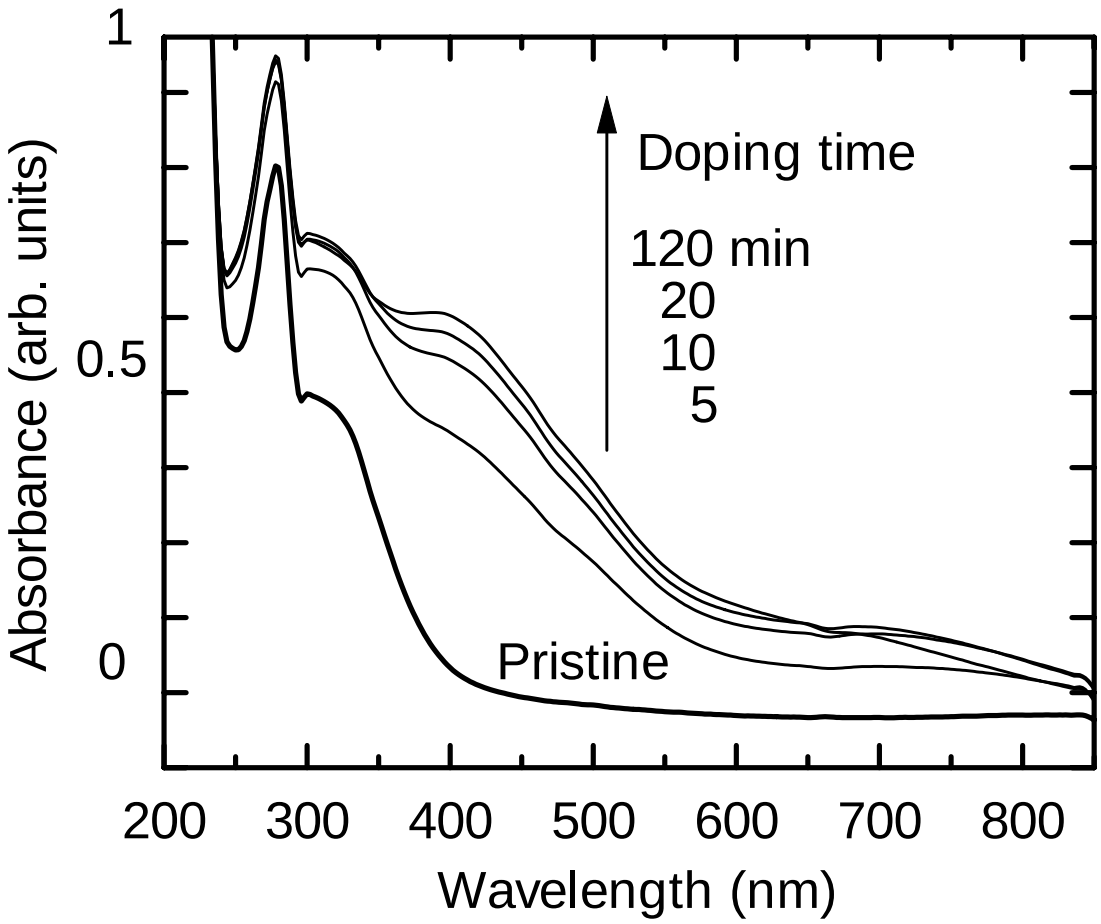


**Figure S6.** *In-situ* UV-vis absorption spectra for PPCH503A(Rh) polymer doped with iodine in the gas phase.

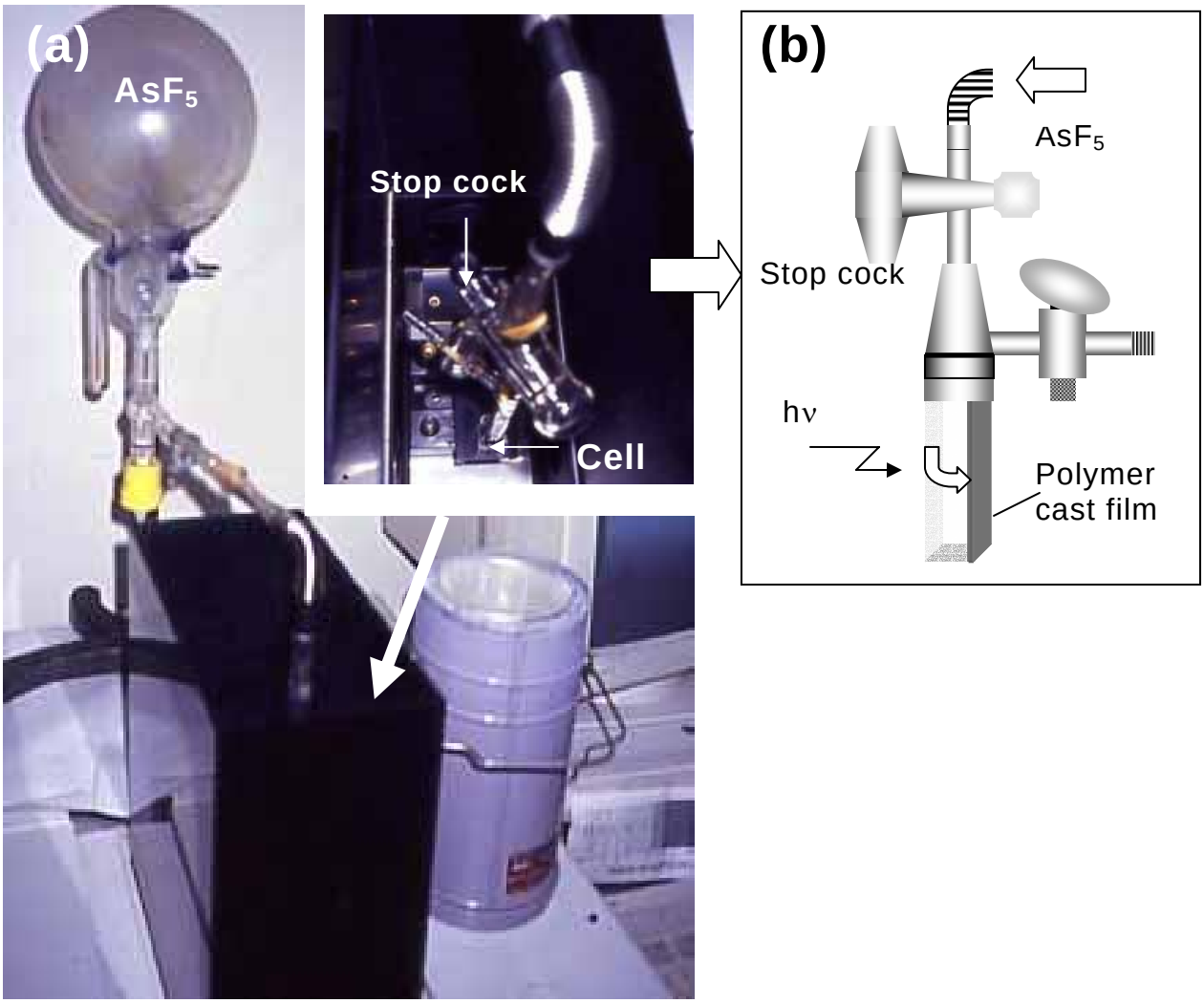


**Figure S7.** Photographs of *in-situ* doping apparatus with UV-vis spectroscopy: (a) doping chamber, and (b) doping cell.

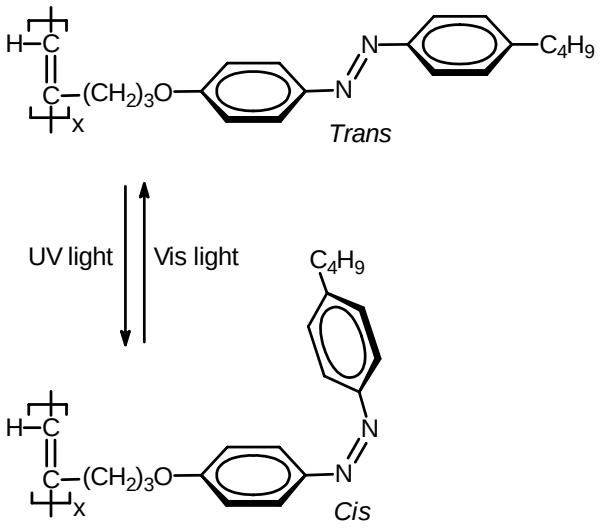
H–C
C–(CH2)3O
X
N
N
C4H9
Trans
UV light
Vis light
C4H9
H–C
C–(CH2)3O
X
N
N
Cis

**Scheme S1.**

## *Synthesis and characterization data*

***5-(4-trans-4'-n-ethylcyclohexyl)phenoxy-1-pentyne*** **(PCH203A)**

This compound was prepared using a method similar to that described for PCH703A. Anal. Calcd. for $C_{19}H_{26}O$: C;. 84.39, H; 9.69. Found: C; 84.13, H; 9.66. IR (KBr, $cm^{-1}$): 3311 ($\nu_{HC\equiv}$), 2120 ($\nu_{C\equiv C}$), 630 ($\delta_{HC\equiv}$). $^{13}C$ NMR (125 MHz, δ from TMS, $CDCl_3$, ppm): 11.55, 15.23, 28.35, 30.04, 33.28, 34.61, 39.15, 43.60, 66.12, 68.77 (H*C*≡C$CH_2$-), 83.58 (HC≡*C*$CH_2$-), 114.33, 127.64, 140.22, 157.03. Mp = 25 °C (no mesophase).

***5-(4-trans-4'-n-Propylcyclohexyl)phenoxy-1-pentyne*** **(PCH303A)**

This compound was prepared using a method similar to that described for PCH703A. Anal. Calcd. for $C_{20}H_{28}O$: C; 84.45, H; 9.92. Found: C; 84.65, H; 9.89. IR (KBr, $cm^{-1}$): 3312 ($\nu_{HC\equiv}$), 2120 ($\nu_{C\equiv C}$), 634 ($\delta_{HC\equiv}$ ). $^{13}C$ NMR (125 MHz, δ from TMS, $CDCl_3$, ppm): 14.39, 15.21, 20.07, 28.32, 33.64, 34.58, 37.03, 39.72, 43.76, 66.11, 68.74(H*C*≡C$CH_2$-), 83.54 (HC≡*C*$CH_2$-), 114.31, 127.59, 140.17, 156.96. Mp = 27 °C (no mesophase).

***5-(4-trans-4'-n-Pentylcyclohexyl)phenoxy-1-pentyne*** **(PCH503A)**

This compound was prepared using a method similar to that described for PCH703A. Anal. Calcd. for $C_{22}H_{32}O$: C, 84.56; H, 10.32. Found: C, 84.34; H, 10.21. IR (KBr, $cm^{-1}$): 3310 ($\nu_{HC\equiv}$), 2121 ($\nu_{C\equiv C}$), 630 ($\delta_{HC\equiv}$). $^{13}C$ NMR (125 MHz, δ from TMS, $CDCl_3$, ppm): 14.10, 15.21, 22.70, 26.68, 28.32, 32.24, 33.70, 34.63, 37.44, 43.76, 66.11, 68.74 (H*C*≡C$CH_2$-), 83.54 (HC≡*C*$CH_2$-), 114.31, 115.02, 127.59, 140.17, 156.96. Transition temperatures: crystal (16 °C) nematic (21 °C) isotropic.

***5-(4-trans-4'-n-Hexylcyclohexyl)phenoxy-1-pentyne*** **(PCH603A)**

This compound was prepared using a method similar to that described for PCH703A. Anal. Calcd. for $C_{23}H_{34}O$: C; 84.60, H; 10.50. Found: C, 84.85; H; 10.52. IR (KBr, $cm^{-1}$): 3314 ($\nu_{HC\equiv}$), 2120 ($\nu_{C\equiv C}$), 628 ($\delta_{HC\equiv}$). $^{13}C$ NMR (125 MHz, δ from TMS, $CDCl_3$, ppm): 14.13, 22.73, 27.01, 29.73, 30.93, 32.00, 32.11, 33.73, 34.66, 37.40, 37.52, 43.60, 67.01 (H*C*≡C$CH_2$-), 83.56 (HC≡*C*$CH_2$-), 114.37, 126.45, 127.61, 140.07, 157.23. Transition temperatures: crystal (21 °C) nematic (23 °C) isotropic.

*6.* ***5-(4-trans-4'-n-Octylcyclohexyl)phenoxy-1-pentyne*** **(PCH803A)**

This compound was prepared using a method similar to that described for PCH703A. Anal. Calcd. for $C_{25}H_{38}O$: C, 84.69; H, 10.80. Found: C, 84.51; H, 10.79. IR (KBr, $cm^{-1}$): 3312 ($\nu_{HC\equiv}$), 2120 ($\nu_{C\equiv C}$), 636 ($\delta_{HC\equiv}$). $^{13}C$ NMR (125 MHz, δ from TMS, $CDCl_3$, ppm): 14.10,

15.21, 22.70, 26.70, 28.32, 29.37, 29.66, 30.01, 31.94, 33.70, 34.58, 37.32, 37.44, 43.76, 66.11, 68.74 (H*C*≡C$CH_2$-), 83.54 (HC≡*C*$CH_2$-), 114.26, 127.59, 140.17, 156.96. Transition temperatures: crystal (41 °C) nematic (44 °C) isotropic.

***8-(4-trans-4'-Hexylcyclohexyl)phenoxy-1-octyne*** **(PCH506A)**

PCH506Br was prepared by the method described in the literature (G. Piao, H. Goto, K. Akagi and H Shirakawa, Polymer 39 (1998) 3559). To a solution of PCH506Br (14.3 g, 35 mmol) in 30 mL of DMF and 20 mL of tetrahydrofuran (THF) was added an excess amount of sodium acetylide. The reaction was carried out at 60 °C for 20 h. The color was changed from brown to violet. The reaction was terminated by an adding a small volume of water into the solution. After evaporation, ether was added and organic layer was washed with water several times. Then $CaCl_2$ was added. After removal of $CaCl_2$, ether was evaporated and the residue was recrystallised with ethanol. The white solid obtained was purified with column chromatography, where mixture of $CHCl_2$ and hexane was used as an eluent. PCH506A (1.2 g, 3.5 mmol) was obtained in yield of 10 %. Anal. Calcd. for $C_{25}H_{38}O$: C, 84.69; H, 10.80. Found: C, 84.59; H, 10.89. IR (KBr, $cm^{-1}$): 3298 ($\nu_{HC\equiv}$), 2116 ($\nu_{C\equiv C}$), 640 ($\delta_{HC\equiv}$). $^{13}$C NMR (125 MHz, δ from TMS, $CDCl_3$, ppm): 14.06, 18.32, 22.69, 25.59, 26.65, 28.46, 28.79, 29.21, 32.21, 33.42, 33.66, 34.58, 37.32, 37.39, 43.71, 67.68, 68.16 (H*C*≡C$CH_2$-), 84.51 (HC≡*C*$CH_2$-), 114.23, 127.54, 139.94, 157.16. Transition temperatures: crystal (8 °C) smectic (18 °C) nematic (30 °C) isotropic.

***1-Bromo-10-chlorodecane*** **(1)**

A solution of thienyl chloride (2.2 g, 19 mmol) in 20 mL of $CHCl_3$ and ~ 5mL of pyridine was slowly added to 10-bromodecan-1-ol (5 g, 19 mmol) by pressure equalized dropping funnel at rt. After 5h, the mixture was washed with water several times, extracted by ether, evaporation, and dried in vacuo to afford 5.3 g of colorless oil (yield: ~100 %). The compound was used in the next step without further purification.

***12-Chloro-dodec-1-yne*** **(2)**

1-Bromo-10-chlorodecane (5.2 g, 0.02 mol) in 10 mL of DMF was added to a solution of sodium acetylide [5.3 g (in 18 wt% xylene/light mineral oil), 0.02 mol] at –30 °C. The reaction mixture was allowed to rt. After 24 h reaction, the reaction mixture was washed with water several times, extracted by ether, evaporation, and dried in vacuo to afford 3.1 g of colorless oil (yield: 48 %). The compound was used in the next step without further purification.

***12-para-(trans-4'-pentyl-cyclohexyl) phenoxy-1-dodecyne*** **(PCH5010A)**

A mixture of (4-*trans*-4'-*n*-pentylcyclohexyl)phenol (2.7 g, 11 mmol), 1-bromo-10-chloro-decane (3.7 g, 15 mmol), $K_2CO_3$ (2.1 g, 15 mmol), and KI (2.5 g, 15 mmol) in 30 mL of DMF was refluxed for 72 h under an argon atmosphere. Then the solution was poured into a large amount of acetone, the solution was filtered off, and the filtrate was evaporated. The crude product was washed thoroughly with water, and extracted with ether. The ether layer was dried over $CaCl_2$ overnight. After the organic solution was evaporated, the yellow solid was further purified by recrystallization from ethanol to afford 2.8 g of white powder (yield = 59 %). Anal. Calcd. for $C_{29}H_{46}O$: C; 84.81, H; 11.29. Found: C, 84.87; H; 11.42. IR (KBr, $cm^{-1}$): 3310 ($\nu_{HC\equiv}$), 2110 ($\nu_{C\equiv C}$), 638 ($\delta_{HC\equiv}$). $^{13}$C NMR (125 MHz, δ from TMS, $CDCl_3$, ppm): 14.12, 18.40, 19.01, 22.73, 26.07, 26.68, 28.49, 28.74, 29.17, 29.37, 29.43, 29.51, 29.54, 32.23, 33.68, 34.60, 37.33, 37.41, 43.74 (O*C*$H_2$), 68.0 (H*C*≡C$CH_2$-), 84.78(HC≡*C*$CH_2$-), 114.24 (ph), 127.58 (ph), 139.93 (ph), 157.23 (ph).

***5-(4-Cyano-4'-biphenoxy)-1-pentyne*** **(CB03A)**

This compound was prepared using a method similar to that described for PCH5010A. Quantity used: 4-cyano-4'-biphenoxy (21.3 g, 0.11 mol), 5-chloro-1-pentyne (11.7 g, 0.11 mol), $K_2CO_3$ (15.2 g, 0.11 mol), and KI (1.82 g, 11 mmol), DMF (100 mL). White powder. Yield: 11.2 g (39 %). Anal; Calcd for $C_{18}H_{15}NO$. C: 82.73, H: 5.79, N: 5.36, found: C: 82.66, H: 5.75, N: 5.33. IR (KBr, $cm^{-1}$): 3257 ($\nu_{HC\equiv}$), 2225 ($\nu_{CN}$), 692 ($\delta_{HC\equiv}$). $^1$H NMR (500 MHz, $CDCl_3$, δ from TMS, ppm): 1.97 (t, *J* = 2.6 Hz, 1H, *H*C≡), 2.03 (quint, *J* = 6.4 Hz, 2H, C*H*$_2$$CH_2$≡CH), 2.42 (dt, *J* = 2.7 Hz, 2H, HC≡CC*H*$_2$), 4.12 (t, *J* = 6.2 Hz, 2H, O$CH_2$), 7.01 (d, *J* = 8.1 Hz, 2H, ph), 7.51 (d, *J* = 8.1 Hz, 2H, ph), 7.61 (d, *J* = 8.4 Hz, 2H, ph), 7.68 (d, *J* = 8.3 Hz, 2H, ph). $^{13}$C NMR (125 MHz, $CDCl_3$, δ from TMS, ppm): 15.13, 28.10, 66.29, 68.97 (H*C*≡C$CH_2$-), 83.01 (HC≡*C*$CH_2$-), 110.15, 115.12, 119.07, 127.11, 128.36, 131.57,132.57, 145.24, 159.55.

***4-Pent-4-ynyloxy-benzaldehyde*** **(3)**

This compound was prepared using a method similar to that described for PCH5010A. Quantity used: 5-chloro-1-pentyne (10 g, 97.5 mmol), *4*-hydroxy benzaldehyde (11.9 g, 97.5 mmol), $K_2CO_3$ (13.47, 97.5 mmol), KI (16.19, 97.5 mmol). Anal. Calcd. for $C_{12}H_{12}O_2$: C, 76.57; H, 6.43;. Found: C, 76.12; H, 6.47. $^1$H NMR (500 MHz, $CDCl_3$, δ from TMS, ppm): 1.98 (t, *J* = 2.6 Hz, 1H, *H*C≡), 1.99-2.16 (m, 4H, C*H*$_2$ x 2), 4.16 (t, *J* = 5.7 Hz, 2H, OC*H*$_2$), 7.01 (d, *J* = 8.7 Hz, 2H, ph), 7.63 (d, *J* = 8.7 Hz, 2H, ph), 9.88 (s, 1H, C*H*O). $^{13}$C NMR (125 MHz, δ from TMS, $CDCl_3$, ppm): 15.11 ($CH_2$), 25.63 ($CH_2$), 67.97 (O*C*$H_2$), 69.20 (H*C*≡C$CH_2$-), 83.05 (HC≡*C*$CH_2$-), 114.80 (ph), 130.02 (ph), 132.00 (ph), 163.97 (ph), 190.77

(*C*HO).

***4-(4-Butyl-phenylazo)-phenol*** **(AB400)**

AB400 was prepared by azo-coupling reaction. Quantity used: 4-*n*-butyl aniline (3.16g, 0.02 mol), 1N HCl (8 mL), $NaNO_2$ (1.5 g), phenol (2 g, 0.02 mol), NaOH (1.3 g in 15 mL $H_2O$). Dark red solid. Yield: 2.3 g (46 %). IR (KBr, $cm^{-1}$): 3360 ($\nu_{OH}$). $^1$H NMR (500 MHz, $CDCl_3$, δ from TMS, ppm): 0.93 (t, *J* = 7.3 Hz, 3H, ph-$CH_2CH_2CH_2CH_3$), 1.37 (sextet, *J* = 7.5 Hz, 2H, ph-$CH_2CH_2CH_2CH_3$), 1.63 (quint, *J* = 7.7 Hz, 2H, ph-$CH_2CH_2CH_2CH_3$), 2.67 (t, *J* = 7.7 Hz, 2H, ph-$CH_2CH_2CH_2CH_3$), 6.94 (d, *J* = 8.6 Hz, 2H, ph), 7.29 (d, *J* = 8.2 Hz, 2H, ph), 7.60 (d, *J* = 8.2 Hz, 2H, ph), 7.87 (d, *J* = 8.6 Hz, 2H, ph). $^{13}$C NMR (125 MHz, δ from TMS, $CDCl_3$, ppm): 13.93, 22.34, 33.43, 35.56, 116.01, 122.52, 125.26, 129.15, 146.13, 146.75, 150.32, 158.87.